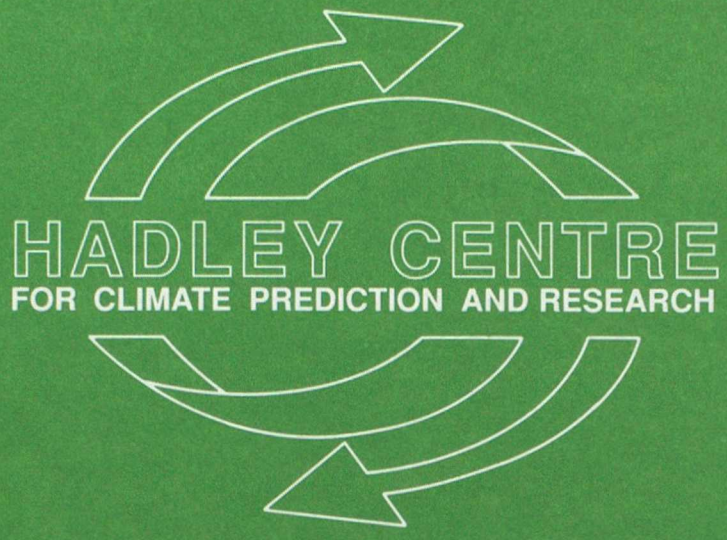

The boreal forests and climate

by

G. Thomas and P. R. Rowntree

CRTN 16

August 1991

CLIMATE
RESEARCH
TECHNICAL
NOTE

Hadley Centre
Meteorological Office
London Road
Bracknell
Berkshire RG12 2SY

CLIMATE RESEARCH TECHNICAL NOTE NO. 16

THE BOREAL FORESTS AND CLIMATE

by

G THOMAS and P R ROWNTREE

Hadley Centre for Climate Prediction and Research
Meteorological Office
London Road
Bracknell
Berkshire RG12 2SY
U.K.

THE BOREAL FORESTS AND CLIMATE

G. Thomas and P. R. Rowntree

Meteorological Office, Bracknell, Berkshire, United Kingdom

(G. Thomas now at Department of Geography, University of British Columbia, 1984--West Mall, Vancouver, V6T 1Z2, B.C., Canada)

ABSTRACT

The sensitivity of modelled northern hemisphere climate to modification of the snow-covered surface albedo is investigated using the United Kingdom Meteorological Office (UKMO) general circulation model. The UKMO GCM is a global, primitive equation model with 11 layers in the atmosphere. Surface processes in the model are highly parameterized, with bulk aerodynamic formulation of the surface fluxes and a "bucket" soil moisture accounting method. The experiment represents in a highly simplified fashion the role of the boreal forests in modulating the surface albedo under snow-covered conditions. A parameterization of snow-covered land was developed which allows the prescription of the maximum albedo attainable with a snow cover to be prescribed as a function of vegetation type. In the standard version of the model the maximum snow-covered surface albedo attainable is 0.60, which exceeds observed values for the forested areas of the northern hemisphere. The sensitivity of the heat and hydrologic budgets for the northern hemisphere and deforested areas is discussed. A detailed analysis of the deforested regions reveals systematic reductions in temperature of up to 2.8 K. Precipitation shows a systematic decrease in the affected regions. The largest decreases occur generally in the months with largest evaporation changes. For the case of no masking by forest vegetation (equivalent to boreal deforestation) the model produces a significant change in the pattern of snowmelt. The removal of forest affects both the magnitude and the timing of spring snowmelt, and consequently also the runoff. There are delays in snowmelt-induced runoff peaks by a month and increases in the magnitudes by on average 32%. A realistic representation of the snow-covered surface albedo is evidently a requirement for simulations of the northern hemisphere climate.

1. INTRODUCTION

The broad-scale distribution of terrestrial ecosystems is widely regarded as being an important component of the global climate system. The exchanges of both energy and materials between the land surface and the atmosphere are influenced by the presence and nature of vegetation (e.g. Rosenzweig and Dickinson, 1986). As a result of the rapidity and extent of contemporary transformations of the earth's surface greater understanding of the potential biotic influences on the climate is urgently required. Recently numerical climate models have been applied to this general problem, focusing particularly on the atmospheric sensitivity to tropical deforestation and semi-arid desertification (e.g. Cunnington and Rowntree, 1986; Dickinson and Henderson-Sellers, 1988). However, one of the largest remaining contiguous vegetation formations on the surface of the earth is the northern hemisphere boreal forests covering some 12,000,000 km^2. Extending as a broad band across the continents of North America and Eurasia, these coniferous forests represent an important global natural resource. Not surprisingly therefore, efforts are currently underway to increase understanding of the role of this major biome within the environment. Small-scale observational (e.g. McCaughey, 1981, 1985) and large-scale empirical (e.g. Kauppi and Posch, 1985; Singh and Powell, 1986) and numerical (e.g. Otterman et al., 1984) studies have been undertaken to assess the sensitivity of the boreal forest species to

environmental change and, conversely, the wider implications of forest removal for the environment.

An important forest influence at high latitudes in the northern hemisphere is the moderation of the snow-covered surface albedo due to masking by protruding vegetation. This effect has been well documented at the local scale (e.g. Leonard and Escher, 1968; Robinson and Kukla, 1984) and also more extensively for the northern hemisphere by Robinson and Kukla (1985a). Figure 1 shows the maximum snow-covered surface albedo for the northern hemisphere based on the analysis of DMSP satellite imagery by Robinson and Kukla (1985a). The zones of maximum albedo (i.e. 71–80%) occur over Greenland, the Canadian Arctic, the Great Plains, the Eurasian Arctic, and the Himalayas. The primarily agricultural lands of Europe are also regions of high albedo. The forest influence upon the maximum surface albedo is readily apparent, with values typically in the region 0.21–0.40. However, to date few studies have explicitly considered this forest influence in terms of large-scale, long-term climate variation. Given the apparent influence of anomalous snow cover on global climate (e.g. Yeh et al., 1983; Barnett et al., 1988, 1989) and the search for greater understanding of the causes of climate variation further studies are warranted.

This paper describes a numerical modelling experiment designed to investigate the significance of vegetation masking of snow-covered surface albedo for the northern hemisphere climate. The experimental procedure is outlined in section

2, including details of the climate model, the parametrization of snow-covered surface albedo, and a description of the model predicted snow cover for the control case. Section 3 presents results for the northern hemisphere and the deforested regions. In section 4, the physics responsible for the modelled response is discussed. In section 5, the results of the experiment are summarised and the conclusions presented.

2. EXPERIMENTAL PROCEDURE

(a) Model

The model employed in this sensitivity study, the United Kingdom Meteorological Office General Circulation Climate Model (UKMO GCM), is extensively documented in Slingo (1985). The current version of the model is a global, primitive equation finite difference GCM, with a spatial resolution of 2.5° latitude and 3.75° longitude. The model has eleven layers in the vertical and employs the sigma co-ordinate system. The basic dynamical equations and finite approximations are given in Slingo (1985). The model uses a leapfrog integration scheme with time smoothing and nonlinear diffusion (Saker, 1975). The model was integrated with seasonally varying forcing. The model version used here incorporates a parametrization of the effects of orographic gravity wave drag. This and other major features of the model are further described in Slingo and Pearson (1987).

Physical processes parametrized in the standard version of the model include: convection and condensation; bulk aerodynamic formulation of the fluxes of sensible heat and latent heat; interactions with subgrid-scale motions through horizontal and vertical diffusion; a bucket hydrology; prescribed, zonally averaged cloud; and the treatment of penetrative convection. More recent versions of the model, however, differ significantly in the treatment of surface hydology (e.g. Warrilow et al., 1986) and may incorporate interactive cloud and ocean processes.

The radiative parameterization allows for three layer clouds and a convective tower. The layer clouds are assumed to be one sigma layer in thickness, but the convective tower may occupy more than one sigma layer. The cloud amounts and heights are defined on a 10° latitude grid for mid-January, April, July and October. For annual cycle integrations the amounts are held constant for 15 days on either side of the middle of each month and at other times are linearly interpolated from the values given. The cloud heights are assigned the value from the month which is closest to the model date.

The penetrative convection scheme is based on the concept of parcel theory modified by entrainment or detrainment of environmental air as described by Gregory and Rowntree (1990). Each model layer may produce an ensemble of buoyant plumes of varying characteristics (temperature, humidity, cross-sectional area) starting at one level and extending upwards to different heights depending on their inherent characteristics. As the plume rises any liquid produced by conden-

sation falls as convective precipitation. The model also condenses and precipitates moisture whenever the air at model grid points becomes supersaturated.

The UKMO GCM includes representation of interactive land surface moisture, snow cover and temperature. Soil moisture content (S_m) is increased by rainfall and snowmelt except that any moisture in excess of 15 cm (the "field capacity") is assumed to form runoff; it is decreased by evaporation at the potential rate (E_p) for $S_m \geq 5$ cm but at a reduced rate ($E_p \times S_m/5$) for $S_m < 5$ cm. The model predicts snowfall if the temperature of the lowest model layer is below 273 K. Snowdepth is increased by snowfall reaching the ground and decreased by snowmelt and sublimation. Snow-free surface albedos are prescribed as constants (independent of time or mositure conditions). The global land-cover and soils data archive of Wilson and Henderson-Sellers (1985) has been used to create a geographical distribution of the snow-free land albedo. Considering the importance of the snow-covered land-surface albedo for this study, a more detailed discussion of this parameterization is presented in the following section.

The surface energy balance for each gridpoint is:

$$S^* + \left(F^{\downarrow} - F^{\uparrow}\right) - H - LE - M = 0$$

where S^* is the absorbed solar flux at the surface, $F^{\uparrow}$ is the upward infrared flux, $F^{\downarrow}$ is the downward infrared flux, H is the sensible heat flux, LE is the product of the evaporation rate and a representative value of the latent heat of evaporation

and M is the rate of snowmelt. The surface temperature is a prognostic equation derived from the energy balance equation. The model incorporates a seasonal solar cycle and realistic land/ocean distribution. The surface topography is based on the 1° x 1° surface elevation dataset of Gates and Nelson (1973).

(b) Parameterization of snow-covered land-surface albedo

The modification of terrestrial albedo due to the presence of a snow cover is generally inadequately treated in GCMs (Marshall, 1986). Although observations indicate the variable nature of the snow-covered surface albedo due to a variety of effects such as snow grain size, solar zenith angle, snow depth, vegetation masking, concentration of absorptive impurities in the snowpack and the characteristics of the underlying surface (Warren and Wiscombe, 1980; Robinson and Kukla, 1984; 1985b), few climate models incorporate such functional dependence in a realistic manner. For example, recent global climate model investigations of the influence of snow cover on regional and global climate simply assume an albedo of 0.60 for full snow coverage of land areas (e.g. Barnett et al., 1989). A maximum of this kind has often been used to allow simply for the masking effects of vegetation in models where no geographical distribution of vegetation is specified.

Table 1 lists some of the methods employed in the parameterization of snow-covered land-surface albedo in GCMs (UKMO1 represents the standard

formulation used in all UKMO GCM integrations until recently, UKMO2 is the parameterization developed for this study; GISS is the formulation employed in the Goddard Institute for Space Studies GCM; and GFDL is that in the Geophysical Fluid Dynamics Laboratory GCM). All parameterization schemes require that a snow free land albedo be specified. This is typically a function of the designated land-cover as noted previously. The standard version of the UKMO GCM incorporates a square root snow-depth dependency in the surface albedo calculation through a formulation similar to that employed in the 5–layer model (Slingo, 1982). In common with other parameterizations, the albedo is limited to a maximum value of 0.60. Consequently, the albedo in forested regions will exceed the values observed for the northern hemisphere (typically 0.30–0.45 based on Kukla and Robinson (1985a)). For this study, an alternative parameterization was developed in which explicit account is taken of vegetation masking. The empirical formulation essentially interpolates between the (prescribed) maximum and minimum values associated with a cover type. The GFDL formulation is functionally similar to UKMO1, with A_s set equal to 0.60. A more complex procedure is employed by Hansen et al. (1983) in the GISS GCM which allows for the masking effects of vegetation and snow age. A problem met in comparing modelled and observed snow cover arises from the fact that climate models calculate the water equivalent depth of snow (i.e. the depth of water resulting from a melt of a column of the snow cover) and not the actual snow depth. The ratio of

meltwater volume to initial snow volume may vary from 0.004 for fresh snow to 0.91 for compacted snow (Linsley et al., 1982). To obtain water equivalent snow depth, knowledge of snowpack density is therefore required. Such measurements are not typically available. Figure 2 compares the UKMO, GFDL and GISS formulations for the hypothetical situation of a uniform 0.1 cm day^{-1} increase in water equivalent snow depth. The standard UKMO formulation (UKMO1 in Table 1) and the GFDL procedure are approximately equivalent formulations and produce similar results. The UKMO2 specification is basically an interpolation between two prescribed limits. The GISS formulation incorporates a snow ageing function as well as vegetation masking, but does not require a specified maximum value. As a further test, Figure 3 compares the calculated albedos from the UKMO2 and GISS formulations with some observations from Robinson and Kukla (1984). The latter study reports surface albedo over typical mid-latitude surfaces during the dissipation of a 50 cm deep snow cover. Two surfaces were selected: meadow (Figure 3a) and deciduous forest (Figure 3b). For each surface type, representative maximum snow-covered and winter snow-free albedos were prescribed as required by the UKMO2 formulation. The snow masking depth required by the GISS formulation was set at 2 m for meadow and 35 m for deciduous forest (derived by trial and error). For the generation of Figure 3, a snow density value of 0.3 g cm^{-3} was assumed. The snow depth represents a regional average based on three NOAA Cooperative Observation stations. The

UKMO2 formulation is of course constrained by the observed maximum but is not sensitive to the snow dissipation. This results in an overestimate of surface albedo during successive days. The observations suggest that the error will be larger in the case of low rather than tall vegetation. The GISS formulation exhibits a more realistic albedo change as the snow pack dissipates, but in each case overestimates the maximum initial snow-covered surface albedo. Modifying the snow masking depth parameter results in closer agreement to the maximum but degrades the representation of the albedo during successive days. Clearly neither representation is entirely satisfactory, but both allow for the important effect of vegetation masking.

(c) Experiment

The procedure adopted in the present study consists of adopting the UKMO2 snow-covered surface albedo formulation only at model grid points in the northern hemisphere designated as forest. The location of the forest points is determined on the basis of the model version of the land-cover data archive compiled by Wilson and Henderson-Sellers (1985). The extent of forest in the northern hemisphere is shown in Figure 4. The boreal forests appear as a more or less continuous band across the northern hemisphere continents at a latitude of approximately 60° N.

Two sets of integrations were performed. In the "forested" integrations the snow-covered surface albedo formulation employed at all forested grid points in

the northern hemisphere was based on the UKMO2 formulation described in Table 1. The surface albedo in the presence of snow varies, therefore, between two prescribed limits: the snow-free surface albedo and the maximum possible snow-covered surface albedo specified as 0.35 for all forest points (this ignores variations due to different forest types). For all non-forested points the snow-covered surface albedo formulation was the standard square root dependency formulation (UKMO1) also described in Table 1. The "deforested" integrations represent a sample of standard model integrations in which the UKMO1 formulation was employed at all surface grid points. The experiments can be viewed as representing situations where (a) the Northern Hemisphere has a uniform vegetation cover with maximum albedo cover of 0.60 ("deforested") and (b) similar but some areas are forest with lower maximum albedos ("forested"). The winter months were not expected to produce significant anomalies because of the low solar elevation over the forested regions. However, as solar elevation increases with the approach of spring, the perturbation will become more important. Thus, the model was integrated for the period 1 February to 30 May. In the forested (or control) case, the model was integrated twice, each run starting from different initial conditions and with the appropriate snow-covered surface albedo formulation applied at all forest points. The deforested (or perturbation) case was represented by a selection of 5 samples for the required period from an existing annual cycle integration (Slingo and Pearson, 1987). Results in the form of monthly averages for the perturbation

(P) and control (C) experiments are presented for the northern hemisphere and for four selected limited areas.

(d) Climate simulation

Given the importance of the representation of the snow covered area for this sensitivity study a comparison of the model predicted and observed snow cover extent and depth for the Northen Hemisphere is included. In this paper we utilize NOAA visible band imagery for comparison. The limitations of the available data sets should be noted. Until recently snow cover data was obtained solely from point observations located primarily in the mid-latitudes. Such data suffer from problems of bias due to poor spatial sampling, but provide relatively accurate *in-situ* measurements. Satellite data offer the advantage of global monitoring on a continuous basis of snow depth, water equivalent, areal extent and snow state (wet/dry), but with questionable accuracy. In particular, the interpretation of visible imagery in terms of areal extent is problematic in regions of persistent cloudiness and extensive forest cover. Passive microwave brightness temperatures can be successfully correlated with water equivalent snow depth (e.g. Goodison et al., 1986). However, no validated continental scale data set of interpreted microwave data is available. A recent comparison of four northern hemisphere snow cover data sets (Scialdone and Robock, 1987) suggests a systematic satellite bias towards overestimation of snow extent, especially the southward extent of the

main snow boundary, together with an underestimation in densely forested areas. These limitations prevent a more quantitative comparison between observations and model. Thus our comparison is perforce restricted to an analysis of snow cover extent.

Figure 5 shows the modelled snow depth for March, April and May together with the observed, satellite derived, snow cover frequencies from Matson et al. (1986). The model's 0.5 cm snow water equivalent contour can be compared with the snow cover frequency contours. Typically the 0.5 cm model contour coincides with the 75% contour on the observed map, but over western North America with the 99% contour, indicating a deficiency of model snow cover, and over central Europe with the 50% contour, perhaps suggesting excessive cover, though interpretation is difficult especially in a transition season. The most marked excesses in the model appear to be over central and eastern Asia, where the model's 0.5 cm contour is near the observed 10% contour in places. This is a common problem area in models (Gates et al., 1990). These deficiencies should be taken into account when interpreting the results in later sections.

3. RESPONSE TO DEFORESTATION

The direct effect of the perturbations is to modify the surface albedo and so also the surface energy balance. The dominant terms in the energy balance are shortwave (solar) radiation and the turbulent fluxes of sensible and latent heat.

Forest removal results in an increase in the albedo, the magnitude of which is a function of the predicted snow depth. As a consequence, the absorption of solar radiation is reduced which in turn alters the net radiation balance at the surface. The relative impact on the surface turbulent fluxes of the reduced energy available will determine the climate response. In the following sections, the climate response over the northern hemisphere and for four regions of forest removal are described. The regions are north west Canada (55.0°–65.0° N; 127.5°–116.25° W); eastern Canada (45.0°–55.0° N; 78.75°–67.5° W); north west Russia (60.0°—67.5° N; 26.25°—37.5° E) and central Siberia (55.0°–65.0° N; 97.5°–108.75° E). In each case results for the control, perturbation and resultant differences are presented.

(a) Changes in albedo and surface net radiation

(i) Northern hemisphere

Table 2 shows that the average change in albedo for the northern hemisphere increases to a maximum in March and then decreases. The initial rise can be understood as due to (i) the increasing importance of the snow albedos in higher latitudes as the sun's influence extends northward, (ii) any increase in snow extent due to the albedo change (see 3.2 and Fig. 7); the subsequent decrease in the differences occurs as the snow-covered area diminishes. The effect on the net surface radiation is delayed relative to the albedo changes because of the seasonal

increase in northern hemisphere incoming radiation. The decrease reaches a maximum in April and is still larger in May than it was in February despite the lesser albedo change. The changes in surface net radiation are displayed in Figure 6 for the months of April and May.

(ii) Forest areas

The albedo changes in the selected forest areas are similar to each other in February, when all four are mostly snow covered, but as the snow line retreats northward the differences decrease first in the relatively warmer regions, and eventually in all the areas. By May Regions 2 and 3 have lost most of their snow in both forested and deforested experiments, and albedo differences are small. The differences in net radiation depend both on albedo and the intensity of the solar radiation, so that the largest differences are in the southernmost region (Region 2) in March; in Region 4, where the snow cover persists longest, the changes in net radiation increase steadily from February to April as the solar radiation intensifies.

(b) Snowmelt and snowdepth

(i) Northern Hemisphere

Table 3 shows that the mean snowdepth is a maximum in February and March and declines rapidly thereafter as discussed earlier. The increase in snowdepth as a result of forest removal increases in absolute terms until April and then decreases as snowcover contracts, although as a fraction of that in the control it is

highest in May at 36%. This increase in snowdepth is perhaps the most striking effect of the deforestation. It should be noted that this result is not inconsistent with the common observation that the snow persists longer in forests. The model is effectively considering only the radiatively active snowcover, i.e. that part that affects the albedo. However, the large scale cooling to be expected with deforestation would cause snowmelt to occur more slowly than it would in a forest clearing in the forested case.

Snowmelt rate is also affected: at first it is decreased, but ultimately it must become larger as the remaining snow in the control decreases in extent; this changeover occurs between March and April in the hemispheric mean. Although the accumulated snowmelt in the deforested case is already greater by the end of May, the remaining snowdepth is still more than in the control. This indicates that there has been an increase in snowfall due to the larger fraction of precipitation which falls as snow with the lower temperatures (see 3.3).

(ii) Forest areas

The regional differences in snowmelt are naturally small until snowmelt starts over the forest areas in the forested case-February in Regions 1 and 2, March in Region 3 and April in Region 4. In all four regions the snowmelt has become greater in the deforested case by May. Note that the snowdepths differ at the start of February because the initial data differ for the forested and deforested

samples; however, by March the effects of the snow albedo change dominate the differences, with increases in snowdepth of over 2 cm liquid water equivalent, while the increases are around 4 cm in April in Region 3, and in April and May in Region 1. Figure 7 shows the geographical distribution of these large differences for March, April and May.

(c) Changes in surface temperature

(i) Northern Hemisphere

The surface temperature (Table 4) decreases due to the reduced absorption of solar radiation; the greater snow extent will also contribute when the surface temperature is near the freezing point as snow constrains the temperature to be at or below that level. The cooling is small in February, reaches a maximum in March and then declines slowly as the snow covered area contracts. One might expect the cooling to induce a negative feedback through a decrease of surface longwave heat loss; with a cooling of 0.8 K, the decrease in upward flux will be over 3 Wm^{-2} for temperatures just below freezing point. However, the northern hemisphere mean differences in net surface longwave radiation do not exceed 0.6 Wm^{-2} in any month. Cloud amounts are prescribed so cloud changes are not responsible. The reason must be that there are decreases in downward longwave flux due to lower atmospheric temperatures and (or) decreased water vapour contents.

(ii) Forest areas

The natural variability of temperature on a regional scale is of similar magnitude to the effects of the albedo changes, so it is to be expected that there will be considerable spatial and temporal variations in the cooling. However, only in February is one of the selected regions warmer when deforested. The cooling averaged over the four regions is a maximum, at 2.8 K, in April.

Figure 8 shows the difference in land surface temperature for April and May between the ensemble average of the deforestation (P) integrations and the control run mean (C). In April, both continents are characterised by large areas with temperature reductions exceeding 2 K. These are consistent with the regions of forest removal and correspond to the lower April surface temperature averaged over the northern hemisphere. In May, the cooling over Eurasia remains, whilst the western region exhibits no significant temperature change, although snowdepths are somewhat enhanced (Figure 6). North America retains a region of cooling in the eastern part of the continent, while Alaska is also characterised by temperature reductions exceeding 2 K. These regions also have increased snowdepth (Figure 7).

(d) Evaporation, sensible heat flux and precipitation

(i) Northern Hemisphere

Although the changes in evaporation and sensible heat flux (Table 5) are small,

they are consistently negative due to the smaller amount of energy available from absorbed radiation. The apportionment of the changes between the two, shifts towards the latent heat flux as the temperatures rise as expected from the Penman-Monteith equation (e.g. Rowntree, 1991). There is also a decline in precipitation on average for the 4 month period, which is very similar to that in the evaporation. This is consistent with results of other experiments in which evaporation decreases have been associated with less precipitation (see Mintz, 1984 for a review). Figures 9 and 10 present the geographical distributions of these changes for the sensible and latent heat fluxes in April and May.

(ii) Forest areas

Evaporation changes in the selected regions are mostly well related to the changes in net radiation; as with the hemispheric mean the change in evaporation is an increasing fraction of the net radiation change as temperature rises, increasing from 33% in February to 74% in May. The precipitation changes are mostly consistent with the hemispheric mean changes apart form some small increases in February and March. As with temperature, natural variability contributes to the differences, but generally a relation is evident between the evaporation and precipitation changes with largest decreases generally in the months with largest evaporation changes.

The precipitation differences (Figure 11) between the P and C integrations are characteristically spatially complex. However, in both April and May there is a clear response associated with the regions of forest removal. Precipitation rates are decreased of the order of 0.5-1.0 mm per day over parts of both North America and Eurasia, and increases of over 0.5 mm d^{-1} are mostly confined south of the snowline (Figure 5). An interesting aspect of the experiment is the possibility of a response of the Indian subcontinent to the perturbed surface albedo (e.g. Barnett et al., 1989). Although precipitation is enhanced over India during April, the May precipitation over India and the Indian Ocean near 10° N is reduced by the order of 0.5–1.5 mm d^{-1}. The magnitudes are not inconsistent with those reported by Barnett et al. (1989).

(e) Soil moisture and runoff

(i) Northern Hemisphere

Soil moisture content for the northern hemisphere (Table 6) is only minimally affected: it is somewhat decreased in February and March and increased in April and May. These changes are in accord with the previously described changes in snowmelt, precipitation and evaporation. Runoff changes are also small, being somewhat decreased in February, March and April, but increased during the major period of snowmelt in May. Thus the impact of forest removal has been to delay

the snowmelt peak by one month. Figure 12 shows the April and May changes in runoff.

(ii) Forest areas

The regional differences in soil moisture content are small (generally less than 0.8 cm), since in general the model is close to saturation during these time periods and latitudes. Therefore, it follows that a positive change in the moisture balance at the surface will appear as a change in runoff rather than a change in soil moisture content. There are considerable regional differences in the timing of the switchover from reduced to increased soil moisture as a result of the changes in snowmelt. Region 4 exhibits reduced soil moisture throughout the period of integration. Regions 1 and 3 exhibit an increase in soil moisture in the last month, while Region 2 has positive changes in soil moisture starting as early as March. The expected changes in soil moisture storage may be somewhat counterbalnced by the reduced precipitation which characterises all of the regions in the latter stages of the experiment.

The removal of forest affects both the magnitude and the timing of the peak runoff. Regions 1 and 2 exhibit delays in snowmelt-induced runoff peaks by a month; the magnitudes are increased by 28% and 19% respectively. Regions 3 and 4 also show an increase in the magnitude of the peak monthly runoff (by 11% and 71% respectively), although the peak runoff occurs in the same month in the

perturbation and control experiments. The differences are statistically significant at the 10% level (two-sided test) for Regions 1 and 4; the interannual scatter is too large to obtain significance with this small a sample for Regions 2 and 3. Although the largest value is no doubt partly due to the particular timing of the runoff peak relative to ends of months, the consistency and the large average increase (32%) suggest a real increase in peak intensity.

4. PHYSICAL MECHANISMS

To facilitate ellucidation of the physical mechanisms responsible for the observed changes, the difference results for each of the previously identified regions are presented graphically.

(a) Heat budget

Figure 13 shows the heat budget differences for the north west Canada (a), eastern Canada (b), north west Russia (c) and Central Siberia regions. A direct consequence of forest removal is an increase in surface albedo, which in turn reduces the absorption of solar radiation at the surface. During the entire spring period, all regions have negative changes in absorbed radiation. The maximum reduction (25–45 W m^{-2}) occurs in March for Eastern Canada and April for the other three regions. The turbulent surface fluxes are also changed, with the latent heat flux exhibiting a large reduction in April in all regions. The maximum impact occurs during March and April (except in north west Russia). During the

early part of the integration this may be somewhat compensated by the reduced energy for snowmelt. Snowmelt tends to be reduced in the early months, but for all regions is enhanced above the control integration by May. Peak snowmelt occurs in March and April. The changes in longwave radiation are a response to the lower surface temperatures, which reduce the upward longwave fluxes in the perturbed simulation. There is also a partly compensating reduction in the emission from the atmosphere due to lower atmospheric temperatures (see 3.3).

(b) Surface hydrology

Figure 14 is a breakdown of the monthly cycle of surface hydrology for each of the previouslty mentioned regions. Precipitation is rainfall plus snowfall. There are substantial changes in surface hydology resulting from forest removal. Precipitation is generally reduced in all months (except north west Canada in March), with the maximum reductions in the range 0.4–0.8 mm d^{-1}. The reductions are greatest in April for all regions apart from eastern Canada (March). The reduced energy available at the surface and the lower temperatures modify the pattern of snowmelt, with a general reduction in the early season snowmelt. Maximum snowmelt differences occur in April and May depending on the region with magnitudes exceeding 0.5–1.0 mm d^{-1}. The influence of snowmelt on the pattern of runoff is apparent. In all regions runoff changes mirror the changes in snowmelt. The soil in the control integration is very close to saturation in all

months and regions (see Table 7). Consequently changes in snowmelt will have maximum impact on runoff.

5. SUMMARY AND CONCLUSIONS

The mechanisims responsible for the pattern of response described in the previous sections can be outlined with reference to the components of the surface energy balance. The primary perturbation of the energy balance is through the surface albedo. The removal of forest in the model allows a higher maximum albedo to be attained with snow cover. In both integrations, the dominant terms in the surface energy balance are the absorbed solar radiation and the latent heat flux. The surface albedo increase consequent upon forest removal results in a reduction in the amount of absorbed solar radiation. Although there is a slight decrease in the net upward longwave radiation, the surface net radiation is reduced by up to 30-50 Wm^{-2} in April and May. The impact of the reduced available energy is clearly evident in the turbulent surface fluxes of sensible and latent heat. The sensible heat flux is reduced by of the order of 10-20 Wm^{-2}. Precipitation shows a systematic decrease in the deforested regions. For the case of no masking by forest vegetation (equivalent to boreal deforestation) the model produces a significant change in the pattern of snowmelt. The removal of forest affects both the magnitude and the timing of spring snowmelt, and consequently also the runoff. There are delays in snowmelt-induced runoff peaks by a month and increases in the monthly peak

magnitudes by on average 32%. There are also anomalous latent heat fluxes in April and May over the northern Indian Ocean. The magnitudes are similar to those reported by Barnett et al. (1989). It is interesting to note that climate model investigations of a possible link between the Asian monsoon and anomalous northern hemisphere climate should take explicit account of the role of surface vegetation cover. A realistic representation of the snow-covered surface albedo is evidently a requirement for simulations of the northern hemisphere climate. The results presented in this paper provide evidence of an important vegetation related feedback operating in the climate system. The presence of large areas of forest in regions that are subject to a seasonal snow cover provides an ameliorating effect on the potential atmospheric forcing due to vegetation masking of the snow. Large-scale forest removal would have a measurable impact on the local climate and also on the surface hydrology.

The results reported here may also be relevant in the context of future climate change. As noted previously, studies have been undertaken to assess the sensitivity of the boreal forest species to climate change. Different forest species can be associated with (statistically) distinct climatic regimes. For example, Singh and Powell (1986) found significant differences in mean monthly temperature and precipitation for three subdivisions of the boreal region of the prairie provinces in Canada. By relating an index of forest activity (e.g. productivity) to the regional climatic index, it is possible to infer the response of the forest groups

to climate change (e.g. Kauppi and Posch, 1985). In reality the relationship of vegetation type to climatic regime is much more complex (involving, for example, the role of competition and disturbance factors) than can be encapusalted by simple regression techniques. Thus the nature of the integrated response of major vegetation groupings to CO_2 induced climate chnage remains considerably uncertain. The projected climate changes in the boreal forest region resulting from direct radiative forcing due to doubled atmospheric CO_2 concentrations indicate increased winter (4°—8° C) and summer (4°—6° C) temperatures and some decreases (generally less than 1 mm d^{-1}) in summer precipitation (Mitchell et al., 1990). Palaeoclimate studies suggest that the boreal forest boundaries in the tundra ecotone may be sensitive to a change of only 1° C (e.g. Prentice, 1986; Woods and Davis, 1989). The magnitude of the projected climate change may thus be beyond the physiological tolerances of the existing vegetation, while the rate of change may be too quick for trees in the south to migrate into the boreal forest zone and for the boreal species to migrate northwards (e.g. Davis, 1989). The consequences could be widespread deforestation, providing a negative feedback to climate change. The data in Table 3 indicate a northern hemispheric surface albedo increase of about 2% for up to 4 months in spring; a smaller effect might be expected in autumn because of the lower solar elevation, giving a northern hemisphere land albedo change of 1% in the annual mean. Since northern hemisphere land is about 20% of the total global surface, the global surface albedo

change would be about 0.2%. The effect on the planetary albedo is about half as large due to the presence of cloud. Consequently the effect on the global heat budget would be a little over 0.3 W m^{-2}, compared with the 4 W m^{-2} from a doubling of CO_2. If the forest areas were merely slow to adjust, there would be changes in the timing of snowmelt in the forest zone as climate warmed, with the melt period over the forest occuring earlier. Clearly the presence and nature of the land-surface cover in extratropical regions has a climatic relevance.

ACKNOWLEDGEMENTS

The initial research for this paper was carried out whilst G. Thomas was supported by a NERC CASE studentship in conjunction with Liverpool University and the U.K. Meteorological Office. R. Wilderspin and D. Warrilow are thanked for their help in setting up the experiments. S. Brentnall aided in the calculation of the statistics and the production of the graphic output from the model.

References

Barnett, T. P., Dumenil, L., Schlese, U. and E. Roeckner, 1988, The effect of Eurasian snow cover on global climate, *Science*, **239**, 504–507.

Barnett, T. P., Dumenil, L., Schlese, U., Roeckner, E. and M. Latif, 1989, The effect of Eurasian snow cover on regional and global climate variations, *J. Atmos. Sci.*, **46**, 661–685.

Cunnington, W. M. and Rowntree, P. R., 1986, Simulations of the Saharan atmosphere-dependence on moisture and albedo, *Q. J. Roy. Met. Soc.*, **112**, 971–999.

Davis, M. B., 1989, Lags in vegetation response to greenhouse warming, *Climate Change*, **15**, 75–82.

Dewey, F. K., 1987, Satellite-derived maps of snow cover frequency for the northern hemisphere, *J. Clim. Appl. Met.*, **26**, 1210–1229.

Dickinson R. E. and Henderson-Sellers, A., 1988, Modeling tropical deforestation, *Quart. J. Roy. Met. Soc.*, **114**(B), 439–462.

Gates, W. L. and A. B. Nelson, 1973, A new tabulation of the Scripps topography on a 1° global grid. Part 1: terrain heights, R-1276–ARPA, Rand Corporation, Santa Monica, California, USA.

Gates, W. L., Rowntree, P. R. and Zeng, Q-C., 1990, Validation of climate models, in, Intergovernmental Panel on Climate Change, *Climate Change, the IPCC Scientific Assessment*, University Press, Cambridge, 93–132.

Goodison, B., Rubenstein, I., Thirkettle, F. W. and Langham, E. J., 1986, Determination of snow water equivalent on the Canadian Praries using microwave radiometry, in, *Modeling Snowmelt Induced Processes*, Proceedings of the Budapest Symposium, July, 1986, IAHS Publ. No. 155, 163–173.

Gregory, D. and Rowntree, P. R., 1990, A mass flux convection scheme with representation of cloud ensemble characteristics and stability dependent closure, *M. Wea. Rev.*, **118**, 1483–1506.

Hansen, J., Russell, G., Rind, D., Stone, P., Lacis, A., Lebedeff, S., Ruedy, R. and Travis, L., 1983, Efficient three-dimensional global models for climate studies: models I and II, *M. Wea. Rev.*, **111**, 609–662

Kauppi P. and Posch, M., 1985, Sensitivity of boreal forests to possible climatic warming, *Climate Change*, **7**, 44–54.

Leonard, R. E. and A. R. Escher, 1968, Albedo of intercepted snow, *Wat. Res. Res.*, **4**, 931–935.

Linsley, R. K., Kohler, M. A. and Paulhus, J. L., 1982, *Hydrology for Engineers*, McGraw-Hill, New York, 508pp.

Marshall, S., 1986, Parameterization of snow albedo for climate models, in, Kukla,

G., Barry, R. G., Hecht, A., Wiesnet, D. (eds.), Snow Watch '85, Proceedings of the workshop held 28–30 October 1985 at the University of Maryland, College Park, MD, Glaciological Data Report GD-18, 215–223.

Matson, M., Ropelewski, C. F. and Varnadore, M. S., 1986, An atlas of satellite derived northern hemisphere snow cover frequency, NOAA ATLAS, NESDIS, Washington, D.C., 75pp.

McCaughey, J. H., 1981, Impact of clearcutting of coniferous forest on the surface radiation balance, *J. Appli. Ecol.*, **18**, 815–826.

McCaughey, J. H., 1985, A radiation and energy balance study of mature forest and clear-cut sites, *Bound.-Layer Met.*, **32**, 1–24.

Mitchell, J. F. B., Manabe, S., Tokioka, T. and Meleshko, V., 1990, Equilibrium climate change, in, Intergovernmental Panel on Climate Change, *Climate Change, the IPCC Scientific Assessment*, University Press, Cambridge, 131–172.

Mintz, Y., 1984, The sensitivity of numerically simulated climates to land-surface boundary conditions, in, Houghton, J. T. (ed.), *The Global Climate*, Cambride University Press, Cambrige, 79–103.

Otterman, J., Chou, M. D. and Arking, A., 1984, Effects of non-tropical forest cover on climate, *J. Clim. Appli. Met.*, **23**, 762–767.

Prentice, I., 1986, Vegetation responses to past climatic variation, *Vegetatio*, **67**, 131–141.

Robinson, D. A. and Kukla, G., 1984, Albedo of a dissipating snow cover, *J. Clim. Appli. Met.*, **23**, 1626–1634.

Robinson D. A. and Kukla, G., 1985a, Maximum surface albedo of seasonally snow-covereed lands, *J. Clim. Appli. Met.*, **24**, 402–411.

Robinson D. A. and Kukla, G., 1985b, Anthropogenic increase of winter surface albedo, *Catena*, **12**, 215–225.

Rosenzweig, C. and Dickinson, R. E., (eds.), 1986, Climate-vegetation interactions, proceedings of a workshop held at NASA/Goddard Space Flight Centre, Greenbelt, Maryland, 1986, 156pp.

Rowntree, P. R., 1991, Atmospheric parameterization schemes for evaporation over land: basic concepts and climate modelling aspects, in, Schmugge, T. J. and Andre, J.-C. (eds.), *Land Surface Evaporation: Measurement and parameterization*, Springer-Verlag, New York, 5–29.

Saker, N., 1975, An 11–layer general circulation model, Met. O. 20 Technical Note II/30, Meteorological Office, Bracknell, 12pp.

Scialdone, J. and Robock, A., 1987, Comparison of northern hemisphere snow cover data sets, *J. Clim. Appl. Met.*, **26**, 53–69.

Singh, T. and J. M. Powell, 1986, Climatic variation and trends in the boreal forest region of western Canada, *Climate Change*, **8**, 267–278.

Slingo, J. M., 1982, A study of the earth's radiation budget using a general

circulation model, *Q. J. Roy. Met. Soc.*, **108**, 379–405.

Slingo, A., 1985, Handbook of the Meteorological Office 11–layer atmospheric general circulation climate model. Volume 1: model description, DCTN 29, Dynamical Climatology, Meteorological Office, Bracknell, Berkshire, 155pp

Slingo, A. and D. W. Pearson, 1987, A comparison of the impact of an envelope orography and of a parameterization of orographic gravity-wave drag on model simulations, *Quart. J. Roy. Met. Soc.*,**113**, 847–870.

Warren, S. G. and W. J. Wiscombe, 1980, A model for the spectral albedo of snow. Part II: snow containing atmospheric aerosols, *J. Atmos. Sci.*, **37**, 2734–2745.

Warrilow, D.A., Sangster, A.B. and Slingo, A., 1986, Modelling of land surface processes and their influence on European Climate, DCTN 38, Dynamical Climatology, Meteorological Office, Bracknell, Berkshire, 92pp.

Wilson, M. F. and Henderson-Sellers, A., 1985, A global archive of land cover and soils data for use in general circulation climate models, *J. Clim., 5,* 119–143.

Woods, K. D. and Davis, M. B., 1989, Palaeoecology of range limits: Beech in the upper Peninsula of Michigan, *Ecology,* **70**, 681–696.

Yeh, T.–C., Wetherald, R. T. and S. Manabe, 1983, The role of snow cover in short-term climatic and hydrologic change, *Mon. Wea. Rev.*, **111**, 1013–1024.

Table 1 Comparison of GCM parameterizations of snow-covered surface albedo for Goddard Institute of Space Studies (GISS), Geophysical Fluid Dynamics Laboratory (GFDL) and the United Kingdom Meteorological Office (UKMO)

$$GISS = A_g + (A_s - A_g)[1 - exp(-ds/ds^*)]$$

$$A_s = 0.5 + 0.35exp(-a_s/5)$$

$$a_s(t + \Delta t) = \{a_s(t) + (1 - a_s(t)/a_\alpha)\Delta t\}exp(-\Delta ds/dc)$$

$$GFDL = A_g + \left((A_s - A_g) \times ds^{0.5}\right) \quad \leq 0.60$$

$$UKMO1 = A_g + 0.38 \times ds^{0.5} \quad \leq 0.60$$

$$UKMO2 = A_g + ((A_s - A_g) \times (1 - exp(-3.7 \times ds)))$$

A_g, A_s are the albedos of snow − free ground and snow of infinite depth
ds, ds are the snow depth and masking depth of vegetation in liquid water equivalent*
a_s is the age in days of the upper snow layer
dc is the snow depth required to refresh snow albedo (0.2 cm)

Table 2 Response of albedo and surface net radiation to forest removal

Albedo (Unit: 0.001)

	FEBRUARY			MARCH			APRIL			MAY		
	C	P	D	C	P	D	C	P	D	C	P	D
R1	211	463	252	185	421	236	150	327	177	120	188	68
R2	227	508	281	198	443	245	144	291	147	131	142	11
R3	242	528	286	237	510	273	165	413	248	132	169	37
R4	239	524	285	241	527	286	234	518	284	140	302	162
NHL	226	242	16	230	253	23	220	241	21	185	197	12

Surface net radiation (Unit: 0.1 W m^{-2})

	FEBRUARY			MARCH			APRIL			MAY		
	C	P	D	C	P	D	C	P	D	C	P	D
R1	-13	-118	-105	341	122	-219	816	558	-258	1250	1128	-122
R2	223	11	-212	599	296	-303	1054	807	-247	1397	1376	-21
R3	-137	-215	-78	200	-16	-216	739	396	-343	1185	1121	-64
R4	-12	-130	-118	315	48	-267	724	293	-431	1231	925	-306
NHL	478	455	-23	724	688	-36	1018	976	-41	1291	1264	-27

Table 3 Response of snowmelt and snow depth to forest removal

Snow depth (Unit: 0.01 cm water equivalent)

	FEBRUARY			MARCH			APRIL			MAY		
	C	P	D	C	P	D	C	P	D	C	P	D
R1	823	826	3	692	947	255	512	879	367	113	475	362
R2	574	734	160	451	679	228	57	297	240	0.2	10	10
R3	832	771	-61	848	874	26	167	587	420	0.03	50	50
R4	791	803	12	868	945	77	738	960	222	129	335	206
NHL	286	295	9	291	318	27	225	266	41	92	125	33

Snowmelt (Unit: 0.01 W m^{-2})

	FEBRUARY			MARCH			APRIL			MAY		
	C	P	D	C	P	D	C	P	D	C	P	D
R1	361	188	-173	440	240	-200	567	463	-104	469	668	199
R2	327	186	-141	654	661	7	392	785	393	13	89	76
R3	17	47	30	766	136	-630	764	1017	253	6	222	216
R4	0	0	0	13	4	-9	747	424	-323	588	1136	548
NHL	75	67	-8	120	95	-25	195	207	12	198	227	29

Table 4 Response of surface temperature to forest removal

Surface temperature (° C)

	FEBRUARY			MARCH			APRIL			MAY		
	C	P	D	C	P	D	C	P	D	C	P	D
R1	-12.1	-15.1	-3.0	-6.8	-9.5	-2.8	-1.0	-2.6	-1.5	6.5	5.3	-1.2
R2	-15.8	-16.8	-1.0	-8.2	-8.8	-0.6	1.1	-1.8	-2.9	8.2	6.4	-1.9
R3	-15.8	-14.7	1.1	-8.8	-11.7	-2.9	1.3	-3.4	-4.7	7.1	6.5	-0.6
R4	-26.1	-27.2	-1.1	-20.5	-23.0	-2.6	-10.4	-12.6	-2.1	3.5	0.6	-3.0
NHL	-0.6	-0.8	-0.2	4.3	3.5	-0.8	10.0	9.4	-0.6	15.6	15.2	-0.4

Table 5 Response of evaporation, sensible heat flux and precipitation to forest removal

Evaporation (Unit:† 0.01 mm d^{-1})

	FEBRUARY			MARCH			APRIL			MAY		
	C	P	D	C	P	D	C	P	D	C	P	D
R1	47	31	-16	93	69	-24	183	138	-45	295	262	-33
R2	60	34	-26	123	80	-43	219	173	-46	323	311	-12
R3	19	11	-8	62	35	-27	176	102	-74	288	270	-18
R4	13	8	-5	50	23	-27	140	76	-64	274	202	-72
NHL	87	83	-4	120	116	-4	182	173	-9	248	241	-7

† 1 mm d^{-1} corresponds to about 29 W m^{-2} for evaporation, 33 W m^{-2} for sublimation

Sensible heat flux (Unit: 0.1 W m^{-2})

	FEBRUARY			MARCH			APRIL			MAY		
	C	P	D	C	P	D	C	P	D	C	P	D
R1	-220	-243	-23	3	-118	-121	199	83	-116	338	290	-48
R2	-17	-120	-103	146	-32	-178	356	199	-157	453	452	-1
R3	-209	-266	-57	-81	-142	-61	126	-30	-156	346	307	-39
R4	-56	-155	-99	141	-37	-178	180	-7	-187	342	194	-148
NHL	208	198	-10	352	330	-22	454	437	-17	543	531	-12

Table 5 (cont) Response of evaporation, sensible heat flux and precipitation to forest removal

Precipitation (Unit: 0.01 mm d)$^{-1}$

	FEBRUARY			MARCH			APRIL			MAY		
	C	P	D	C	P	D	C	P	D	C	P	D
R1	180	166	-14	157	167	10	237	194	-43	311	271	-40
R2	181	146	-35	256	212	-44	290	277	-13	358	352	-6
R3	85	85	0	152	83	-69	251	159	-92	283	263	-20
R4	43	51	8	80	59	-21	194	148	-46	310	280	-30
NHL	149	143	-6	175	177	2	261	248	-13	315	312	-3

Table 6 Response of soil moisture and runoff to forest removal

Soil moisture (Unit: 0.01 cm)

	FEBRUARY			MARCH			APRIL			MAY		
	C	P	D	C	P	D	C	P	D	C	P	D
R1	1484	1450	-34	1488	1454	-34	1470	1461	-9	1403	1417	14
R2	1467	1440	-27	1483	1486	3	1464	1479	15	1397	1411	14
R3	1469	1477	8	1483	1466	-17	1479	1474	-5	1406	1413	7
R4	1303	1224	-79	1305	1241	-64	1371	1302	-69	1460	1456	-4
NHL	768	756	-12	780	775	-5	806	807	1	811	818	7

Runoff (Unit: 0.01 mm d^{-1})

	FEBRUARY			MARCH			APRIL			MAY		
	C	P	D	C	P	D	C	P	D	C	P	D
R1	115	67	-48	125	72	-53	167	131	-36	157	213	56
R2	87	44	-43	236	211	-25	174	281	107	61	92	31
R3	6	18	12	213	44	-169	262	291	29	43	95	52
R4	0	0	0	0.3	0	-0.3	154	78	-76	189	324	135
NHL	47	43	-4	60	53	-7	103	99	-4	125	132	7

Figure Legends

Figure 1 Maximum snow-covered surface albedo of seasonally snow-covered northern hemisphere land (after Robinson and Kukla, 1985a).

Figure 2 Comparison of GCM snow-covered surface albedo formulations for uniform hypothetical snow depth increase (see Table 1 for details of the formulations).

Figure 3 Comparison of UKMO2 and GISS snow-covered surface albedo formulations with observations for two different surface types (a) meadow, (b) deciduous forest.

Figure 4 Specification of forest points in the UK Meteorological Office GCM.

Figure 5 Modelled (cm water equivalent) and observed (frequency of coverage) distribution of snow depth for (a) March, (b) April and (c) May (modelled contours at 0.5, 1.0, 5.0, 10.0, 30.0, 50.0 cm water equivalent; observed contours at 10%, 50%, 75% 99% frequency).

Figure 6 Modelled distribution of changes in surface net radiation (W m^{-2}) for (a) April and (b) May (contours at +/- 10, 20, 30, 50, 100 W m^{-2}, negative values shaded).

Figure 7 The geographical distribution of snow depth changes (cm water equivalent) for (a) March, (b) April and (c) May (contours at +/- 0.5, 1.0, 5.0,

10.0, 30.0, 50.0 cm water equivalent, negative values shaded).

Figure 8 The geographical distribution of temperature changes (K) for (a) April and (b) May (contour interval 1 K, differences of —2 K or more shaded).

Figure 9 The geographical distribution of changes in sensible heat flux (W m^{-2}) for (a) April and (b) May (contours at +/- 10, 20, 30, 50 W m^{-2}, negative values shaded).

Figure 10 The geographical distribution of changes in latent heat flux (W m^{-2}) for (a) April and (b) May (contours at +/- 10, 20, 30, 50 W m^{-2}, negative values shaded).

Figure 11 The geographical distribution of precipitation changes (mm d^{-1}) for (a) April and (b) May (contours at 0.5, 1.0, 3.0, 5.0, 10.0 mm d^{-1}, negative values shaded).

Figure 12 The geographical distribution of runoff changes (mm d^{-1}) for (a) April and (b) May (contours at 0.5, 1.0, 3.0, 5.0, 10.0 mm d^{-1}, negative values shaded).

Figure 13 Components of the heat budget differences (W m^{-2}) for (a) north west Canada, (b) eastern Canada, (c) north west Russia and (d) central Siberia.

Figure 14 Components of the surface hydrology differences (mm d^{-1}) for (a) north west Canada, (b) eastern Canada, (c) north west Russia and (d) central Siberia.

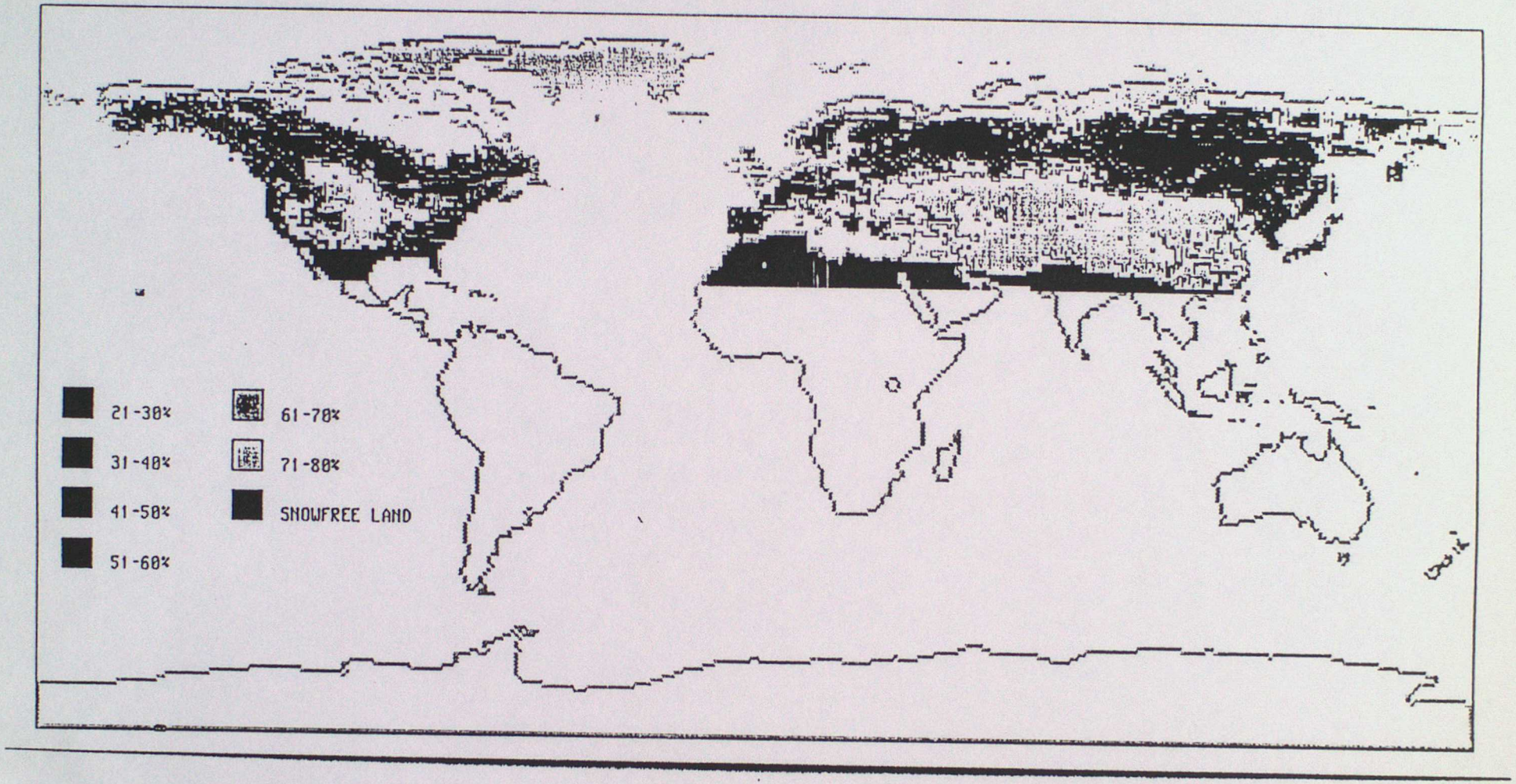

Figure 1

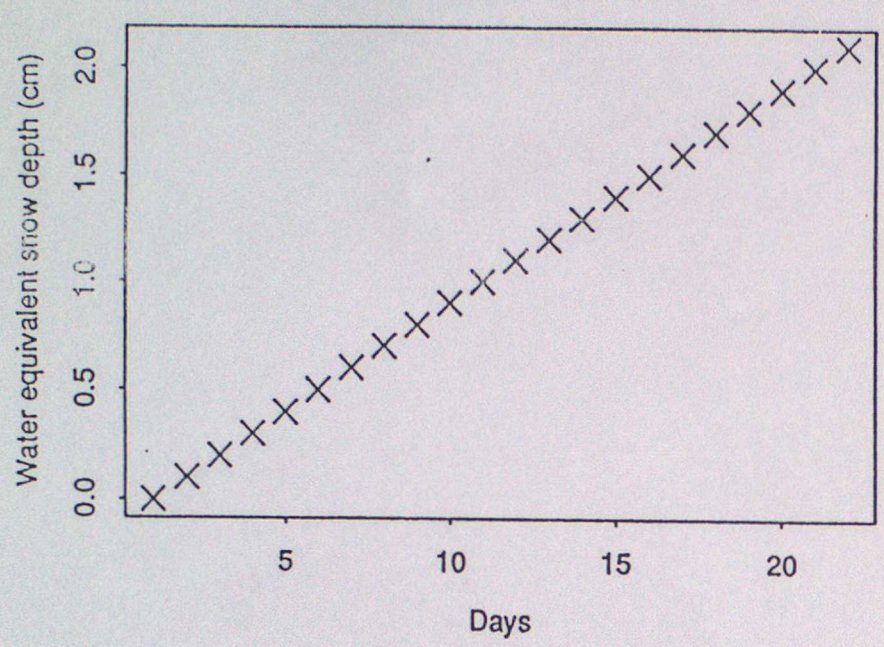
Water equivalent snow depth (cm)
0.0
0.5
1.0
1.5
2.0
5
10
15
20
Days

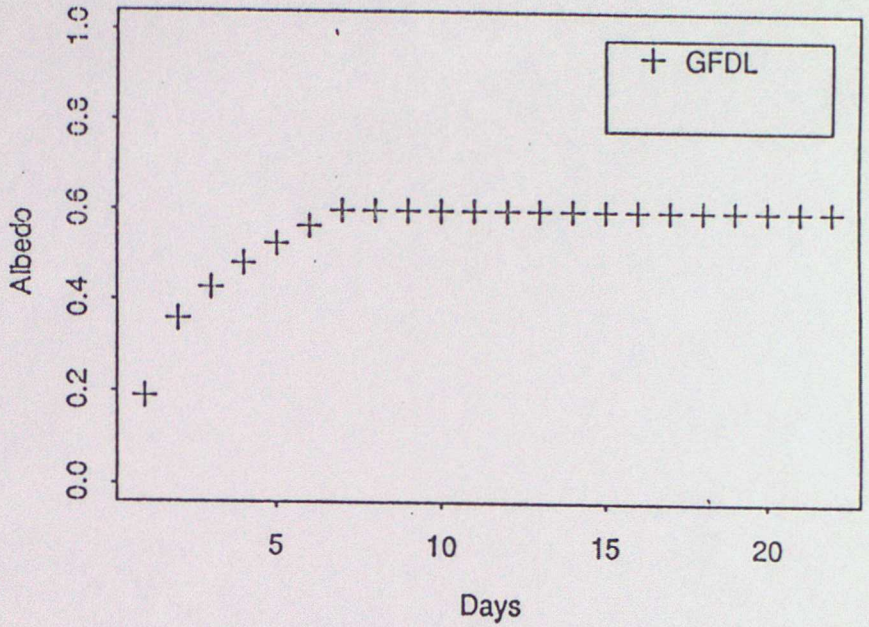
Albedo
0.0
0.2
0.4
0.6
0.8
1.0
GFDL
5
10
15
20
Days

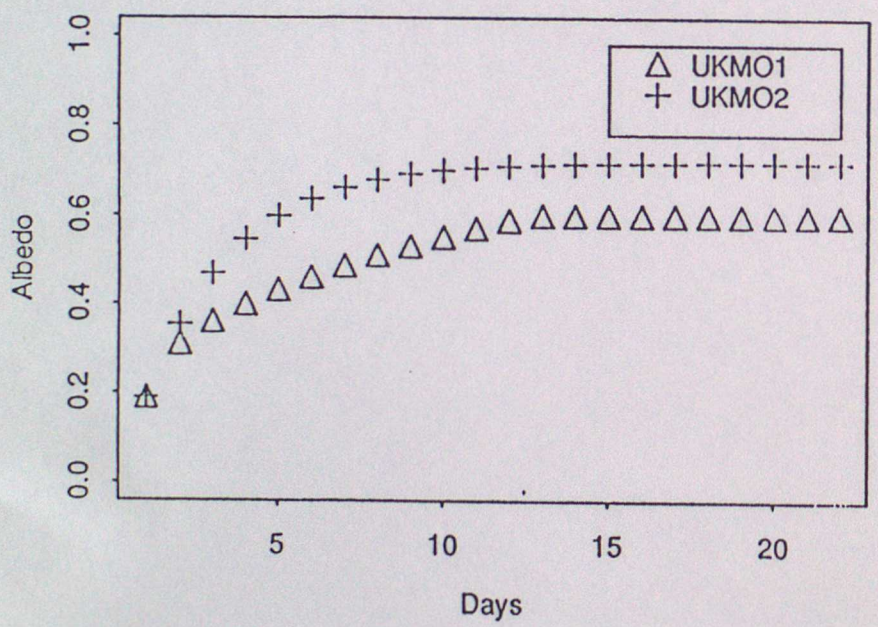
Albedo
0.0
0.2
0.4
0.6
0.8
1.0
UKMO1
UKMO2
5
10
15
20
Days

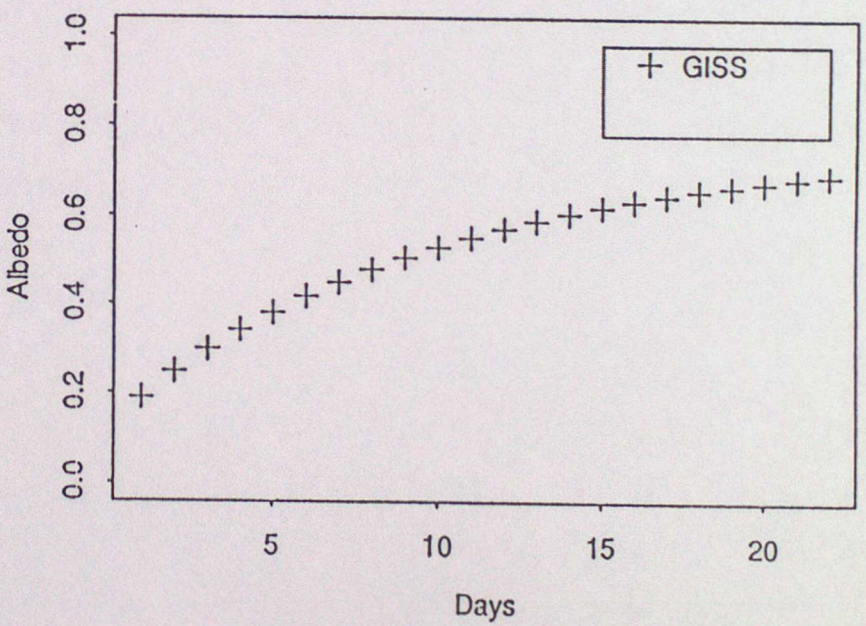
Albedo
0.0
0.2
0.4
0.6
0.8
1.0
GISS
5
10
15
20
Days

Figure 2

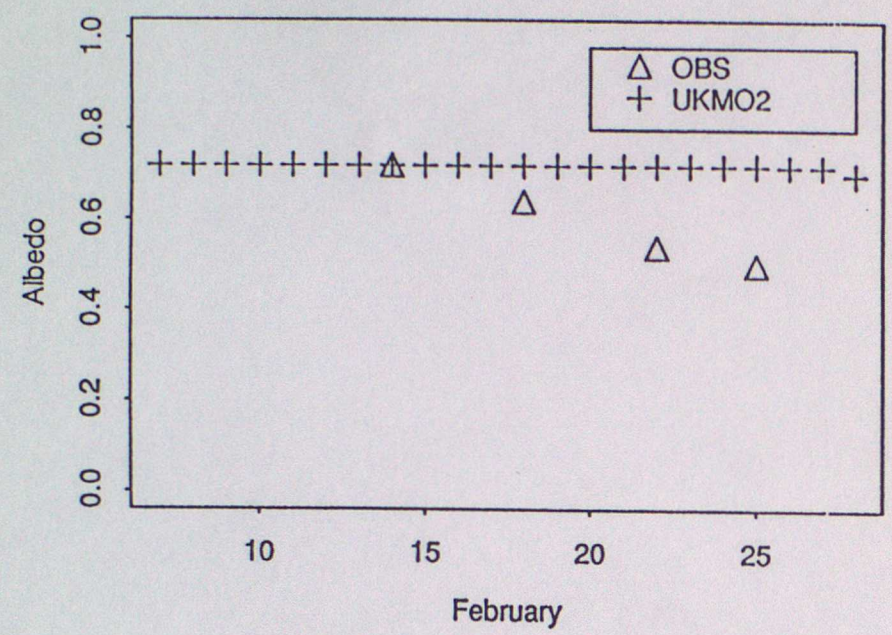
OBS
UKMO2
Albedo
0.0
0.2
0.4
0.6
0.8
1.0
10
15
20
25
February

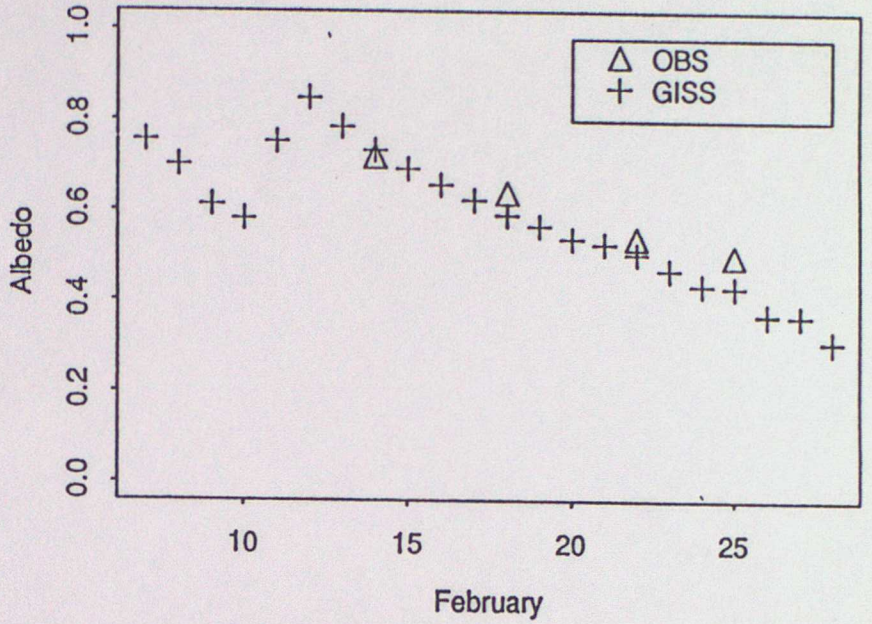
OBS
GISS
Albedo
0.0
0.2
0.4
0.6
0.8
1.0
10
15
20
25
February

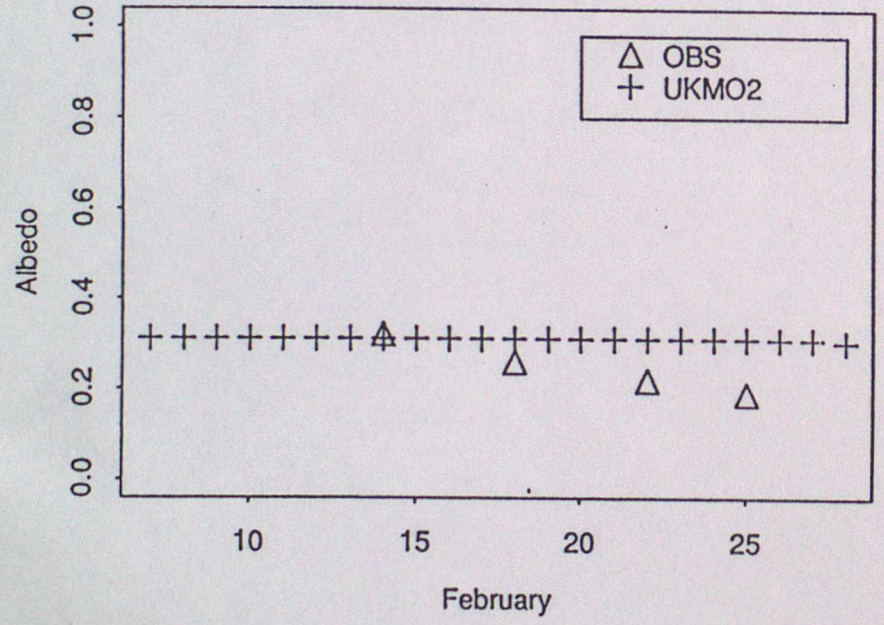
OBS
UKMO2
Albedo
0.0
0.2
0.4
0.6
0.8
1.0
10
15
20
25
February

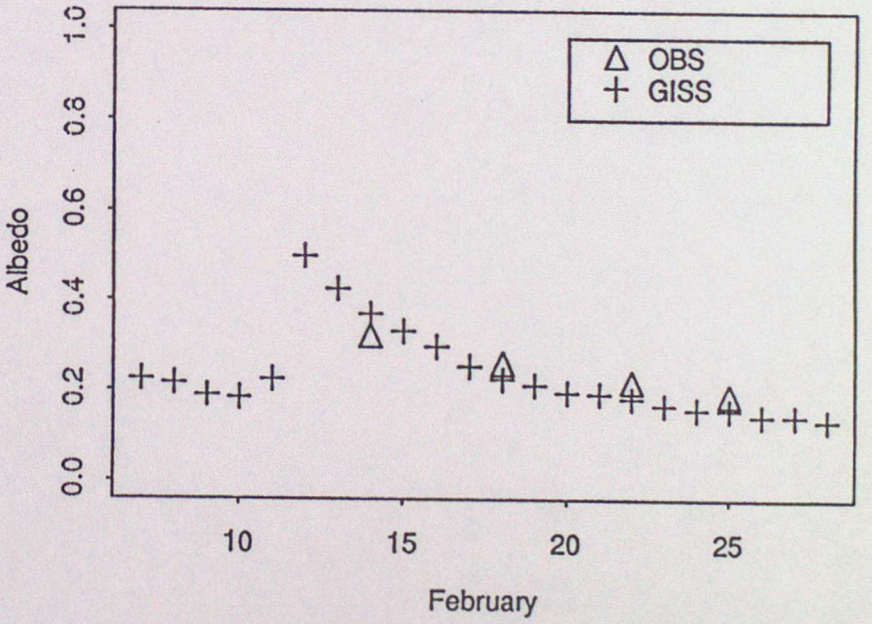
OBS
GISS
Albedo
0.0
0.2
0.4
0.6
0.8
1.0
10
15
20
25
February

Figure 3

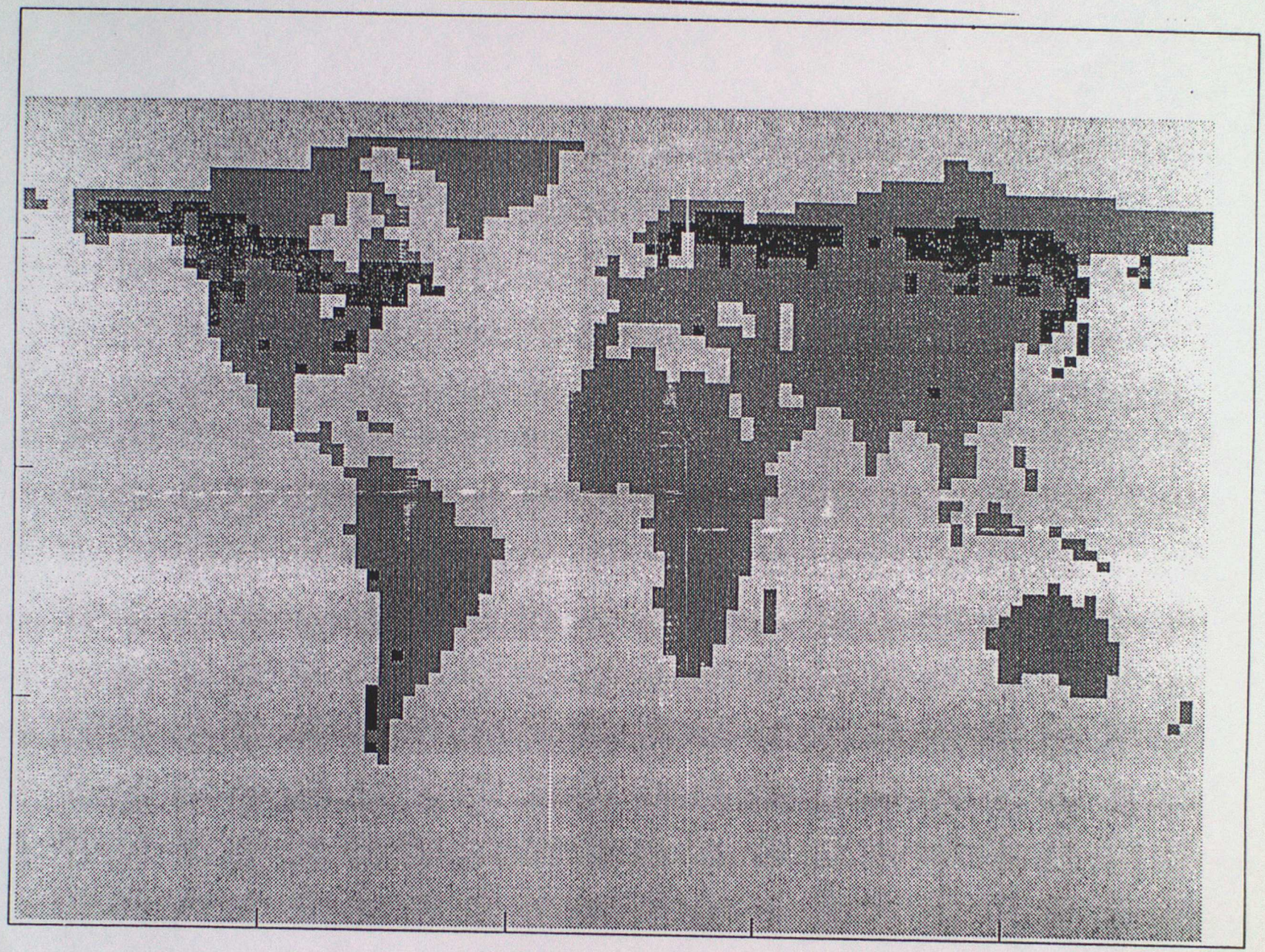

Figure 4

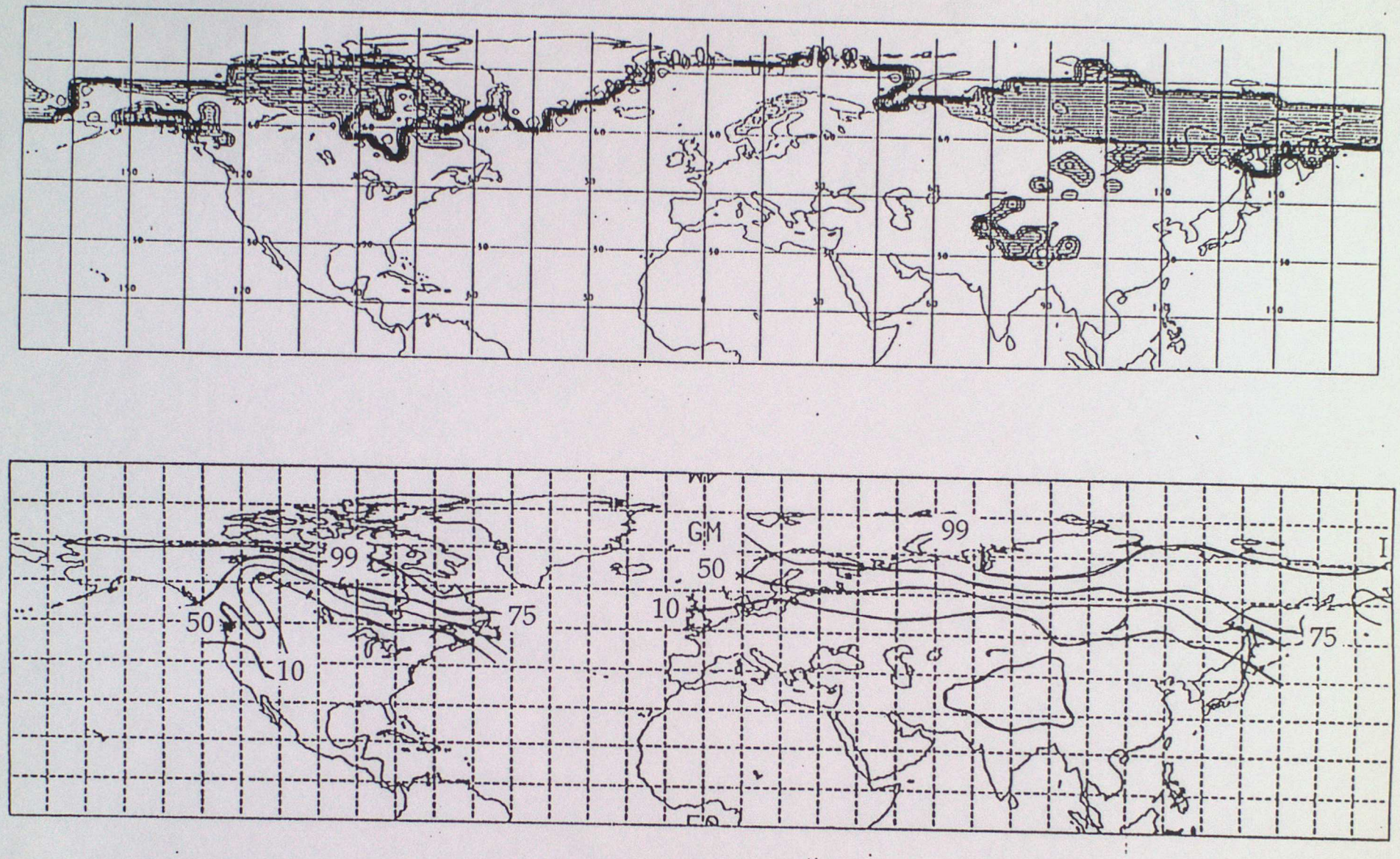

Figure 5a

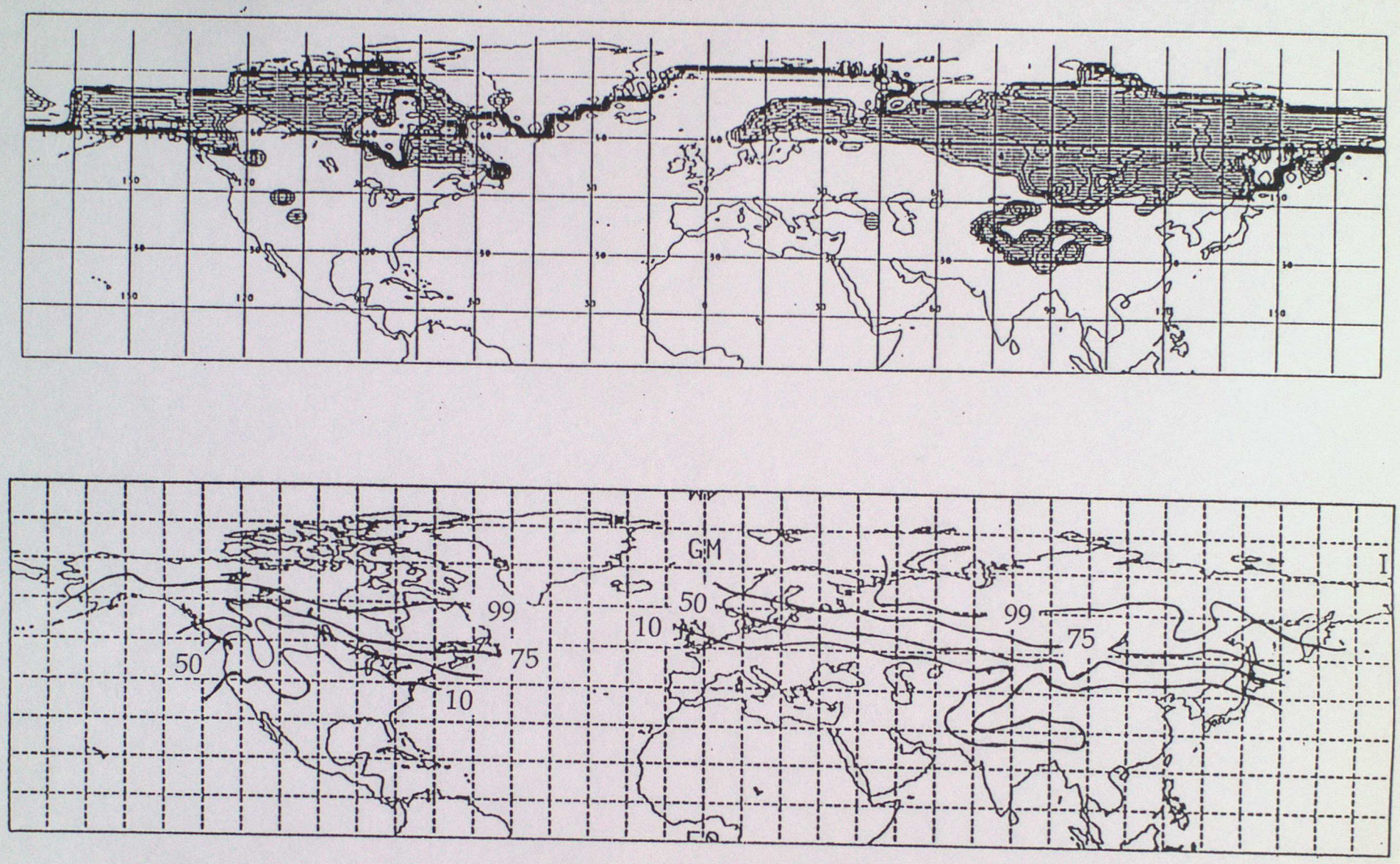

Figure 5b

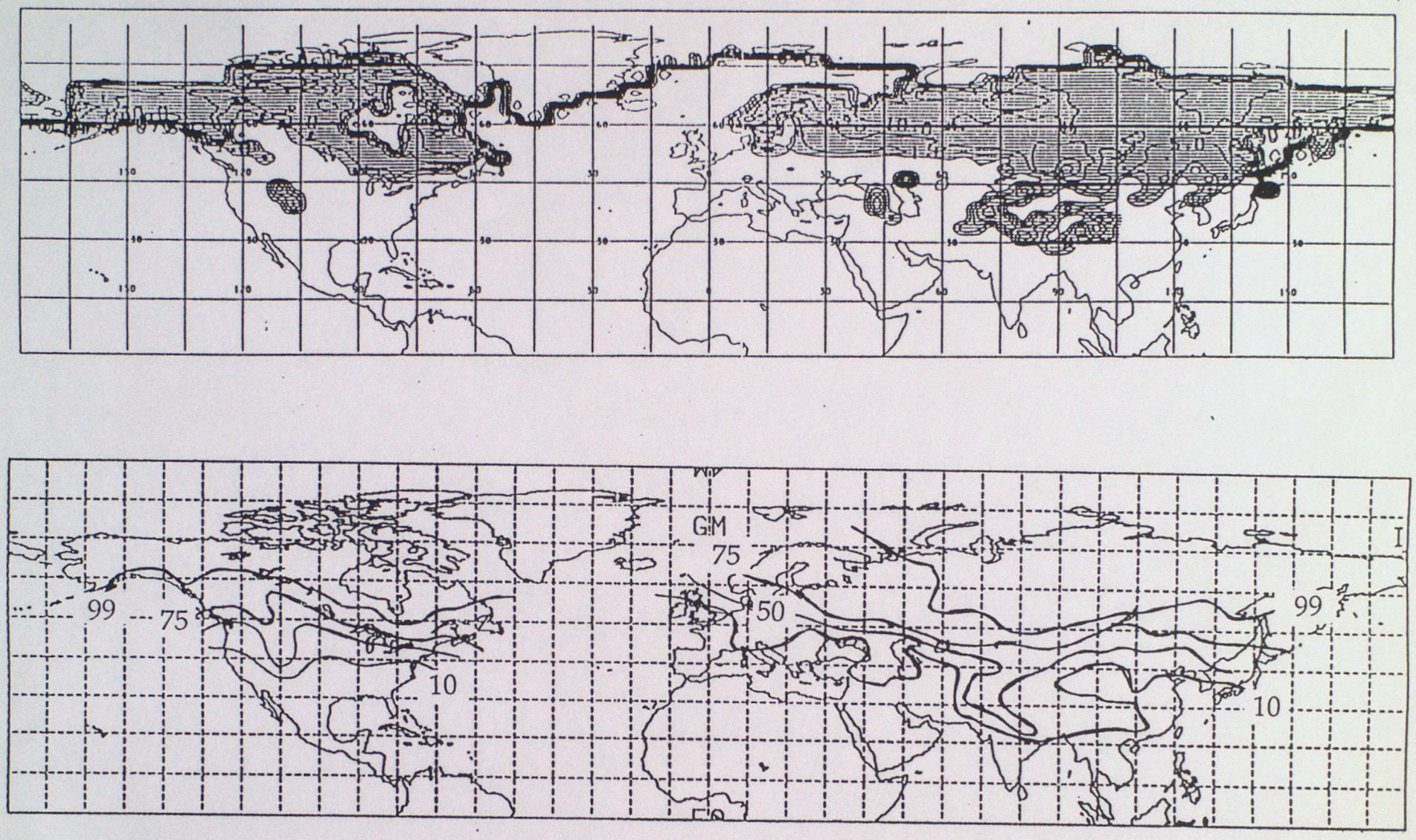

Figure 5c

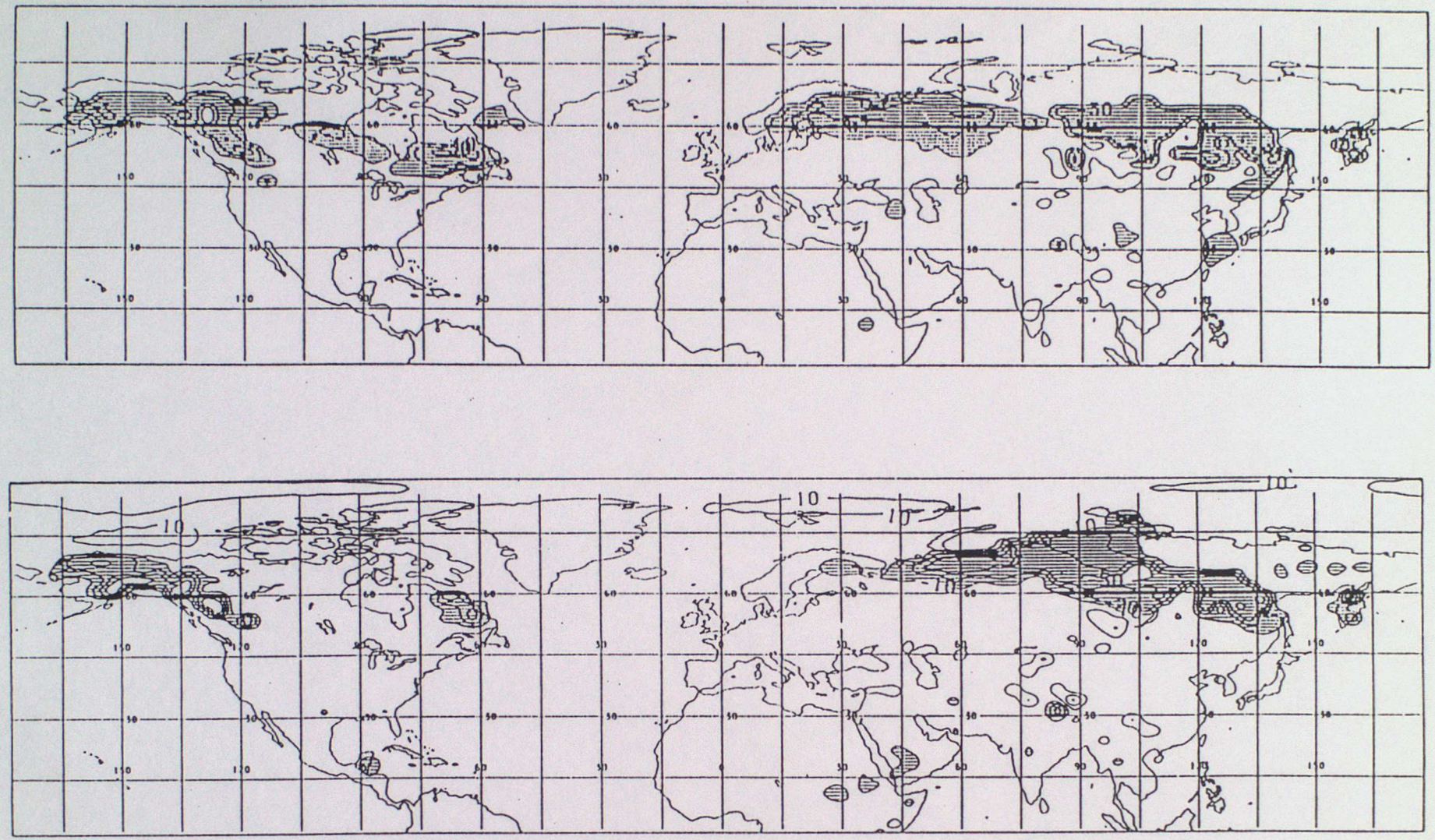

Figure 6

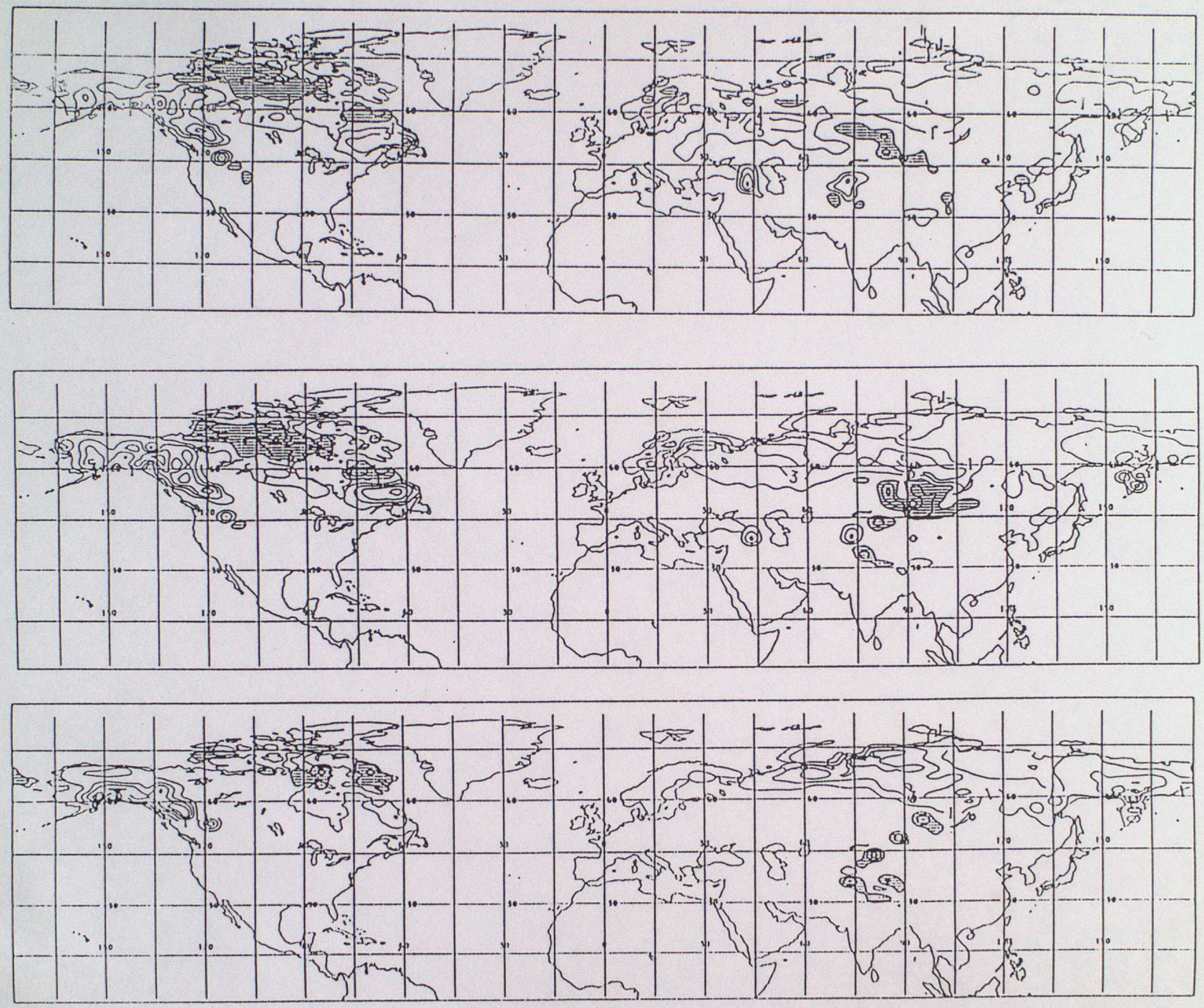

Figure 7

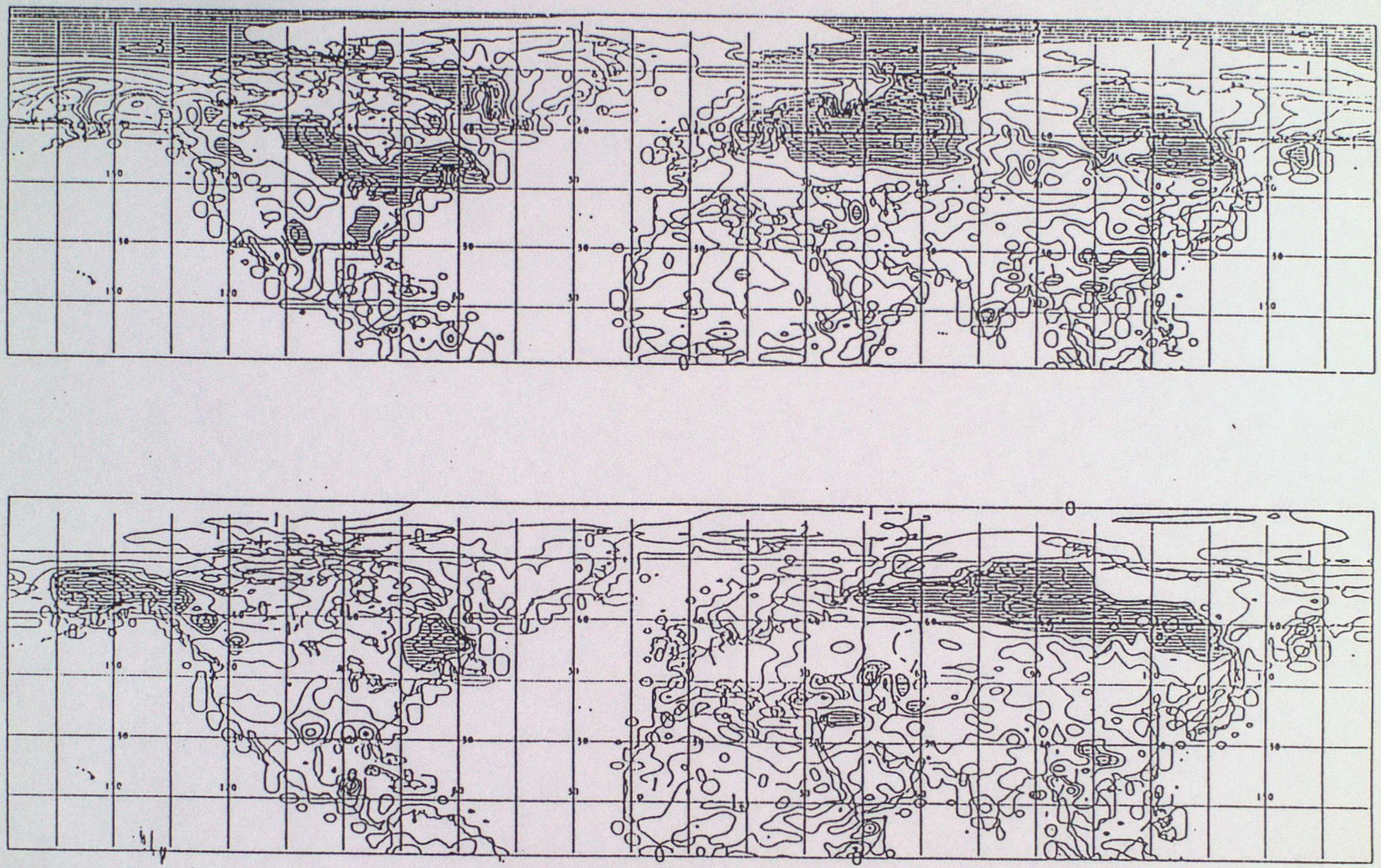

Figure 8

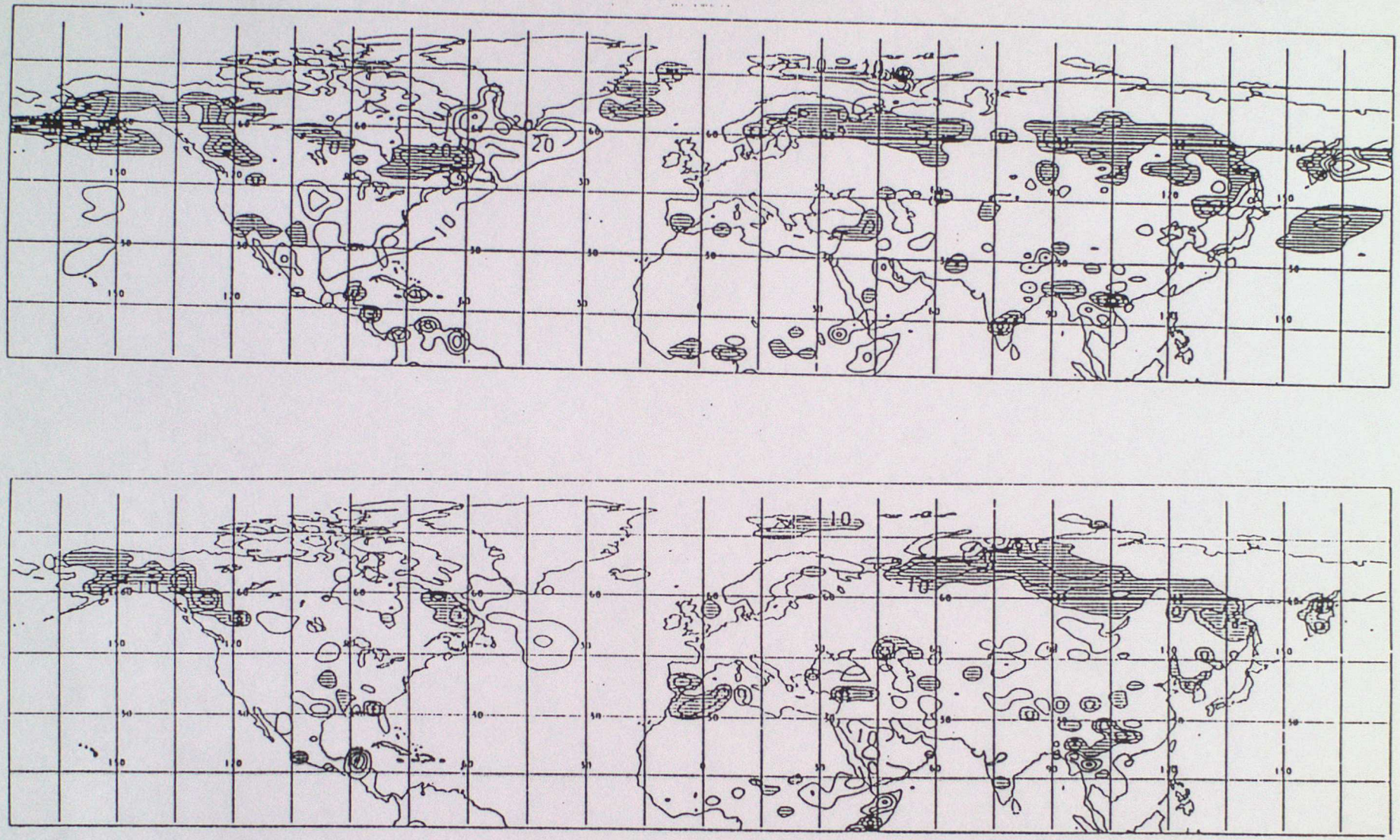

Figure 9

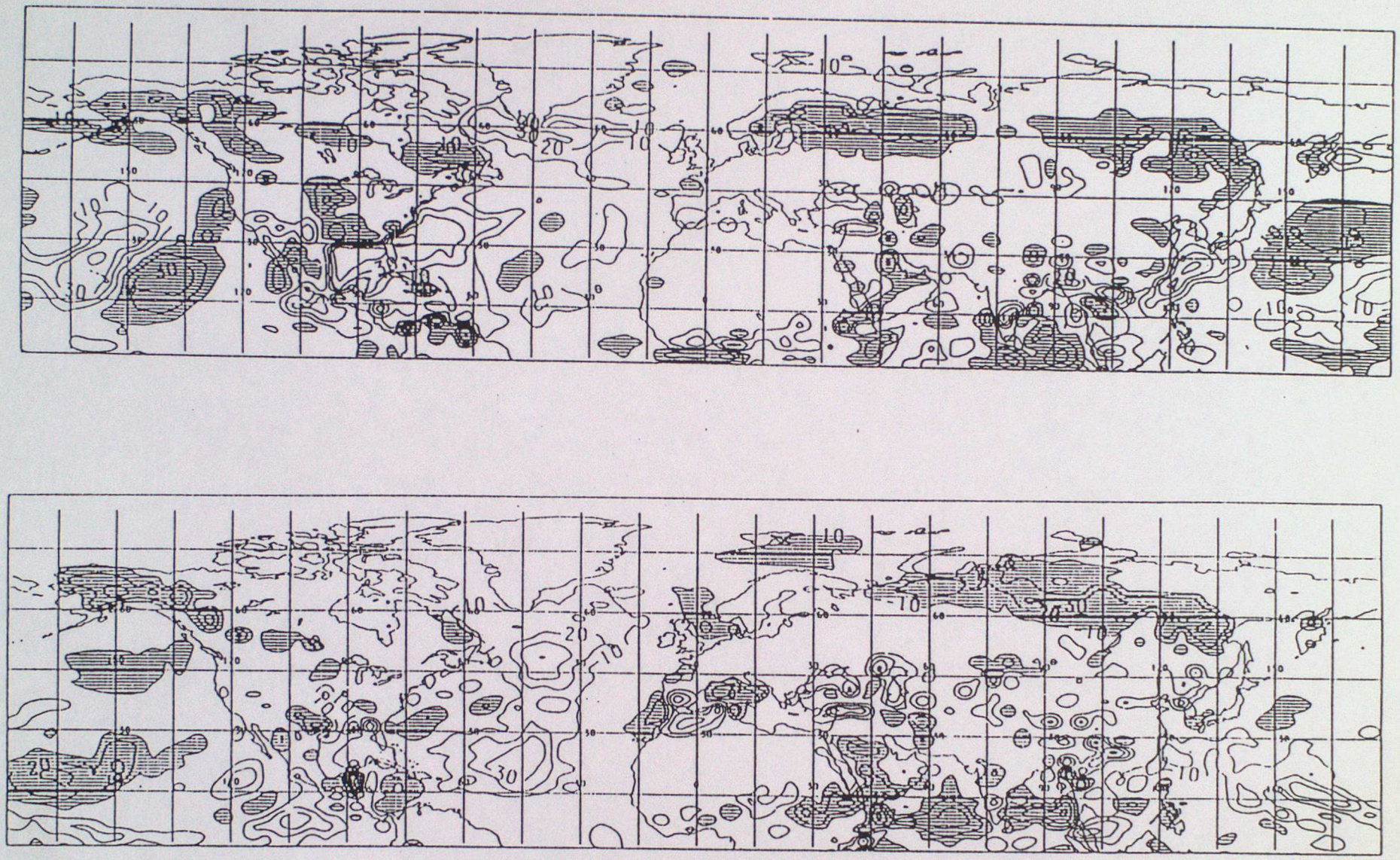

Figure 10

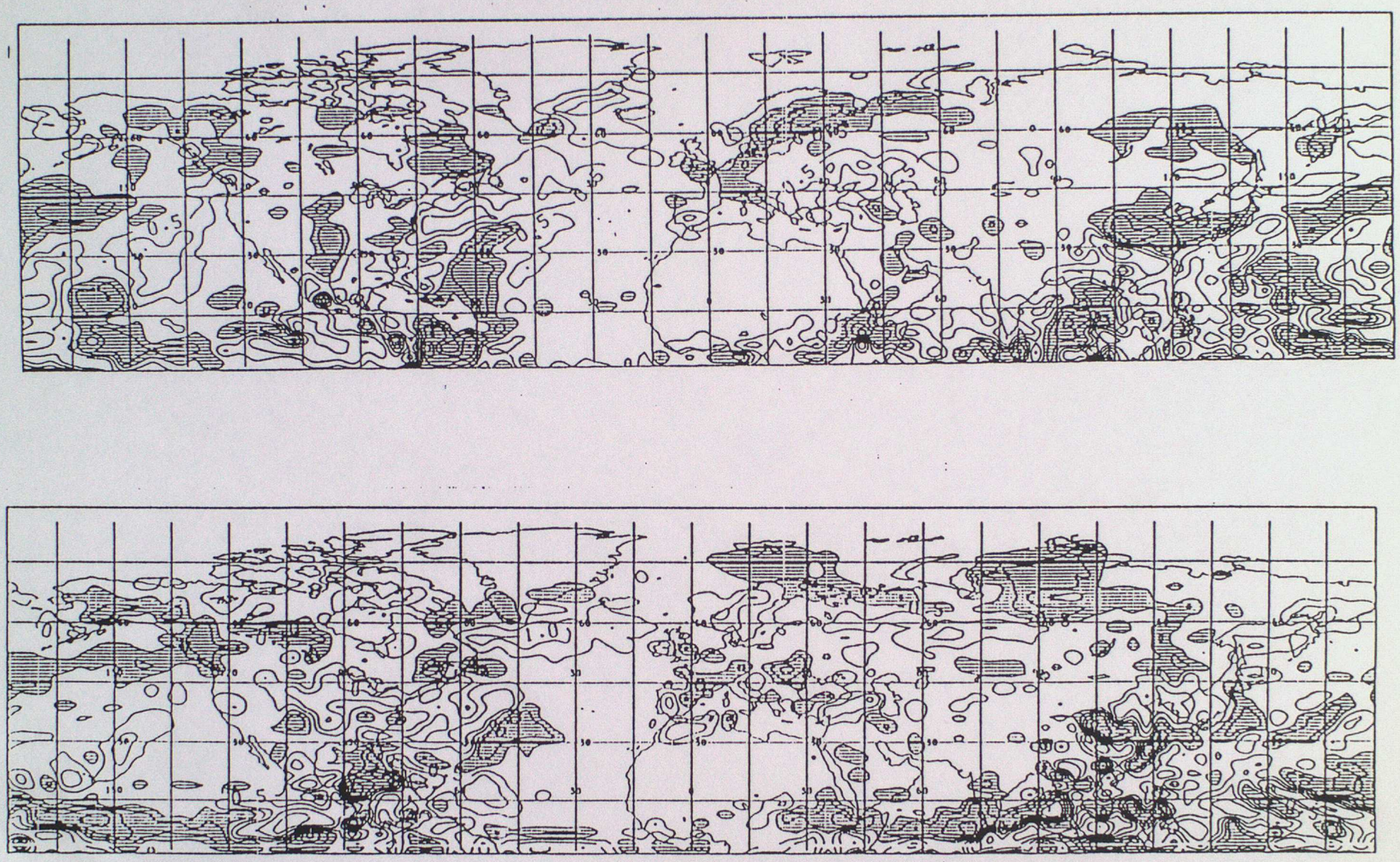

Figure 11

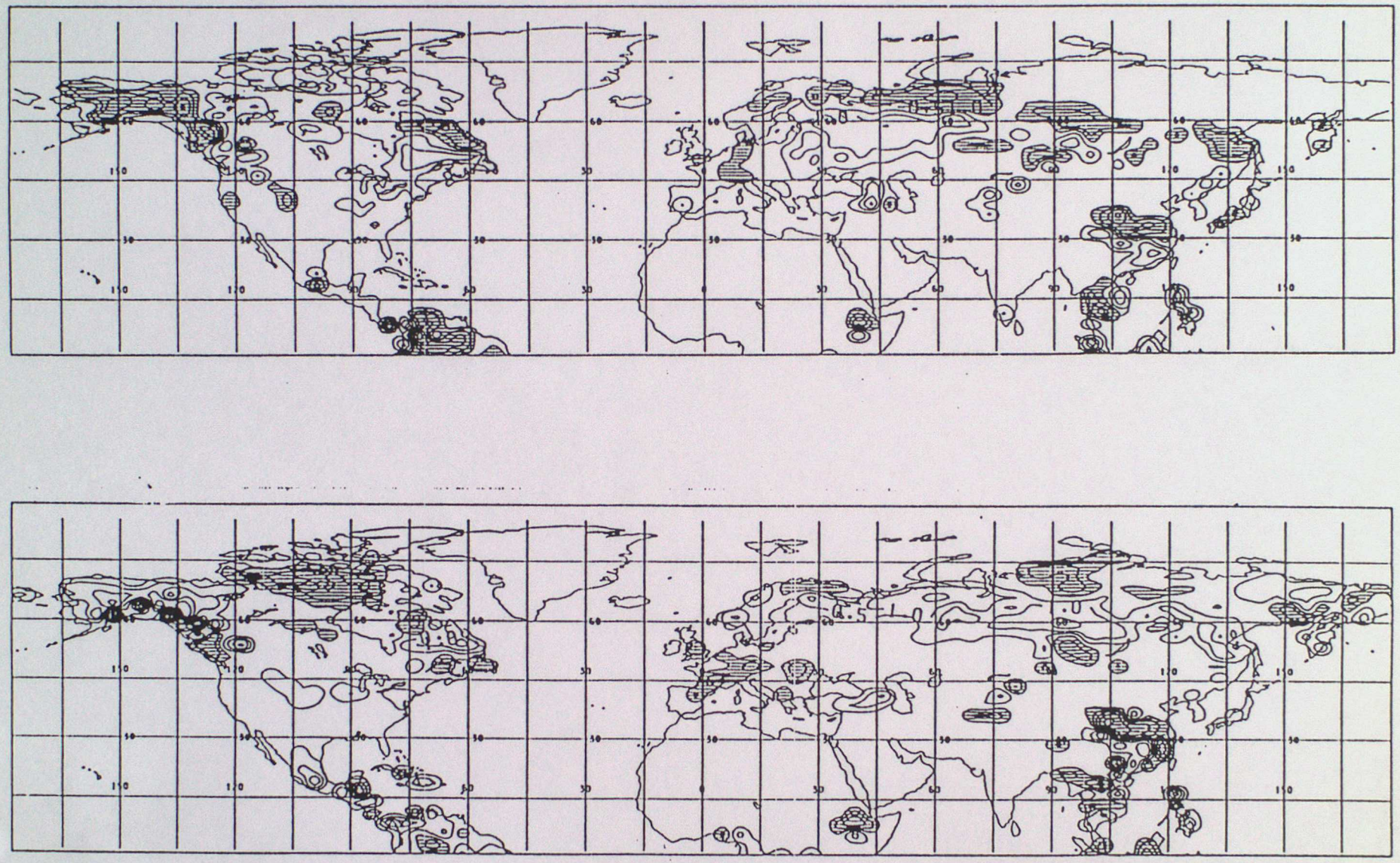

Figure 12

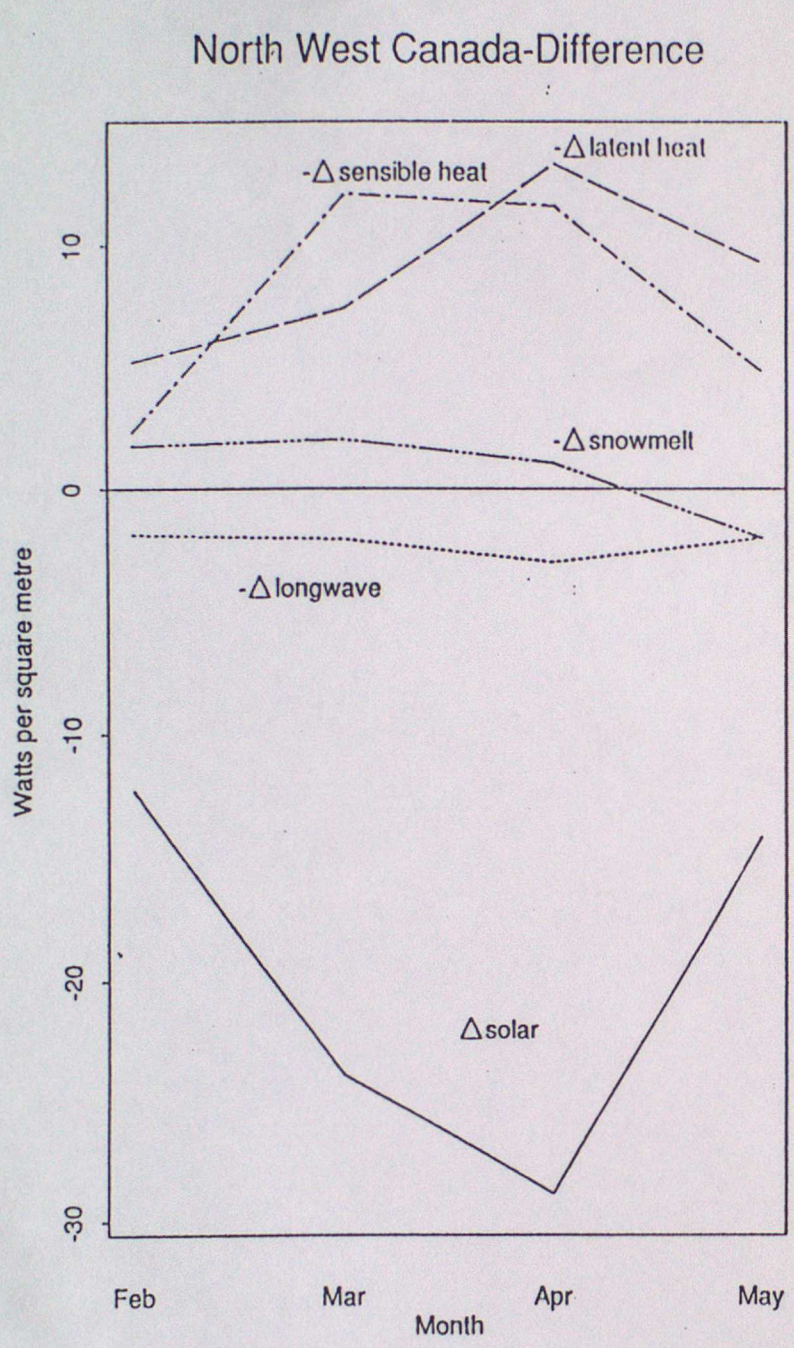

Figure 13a

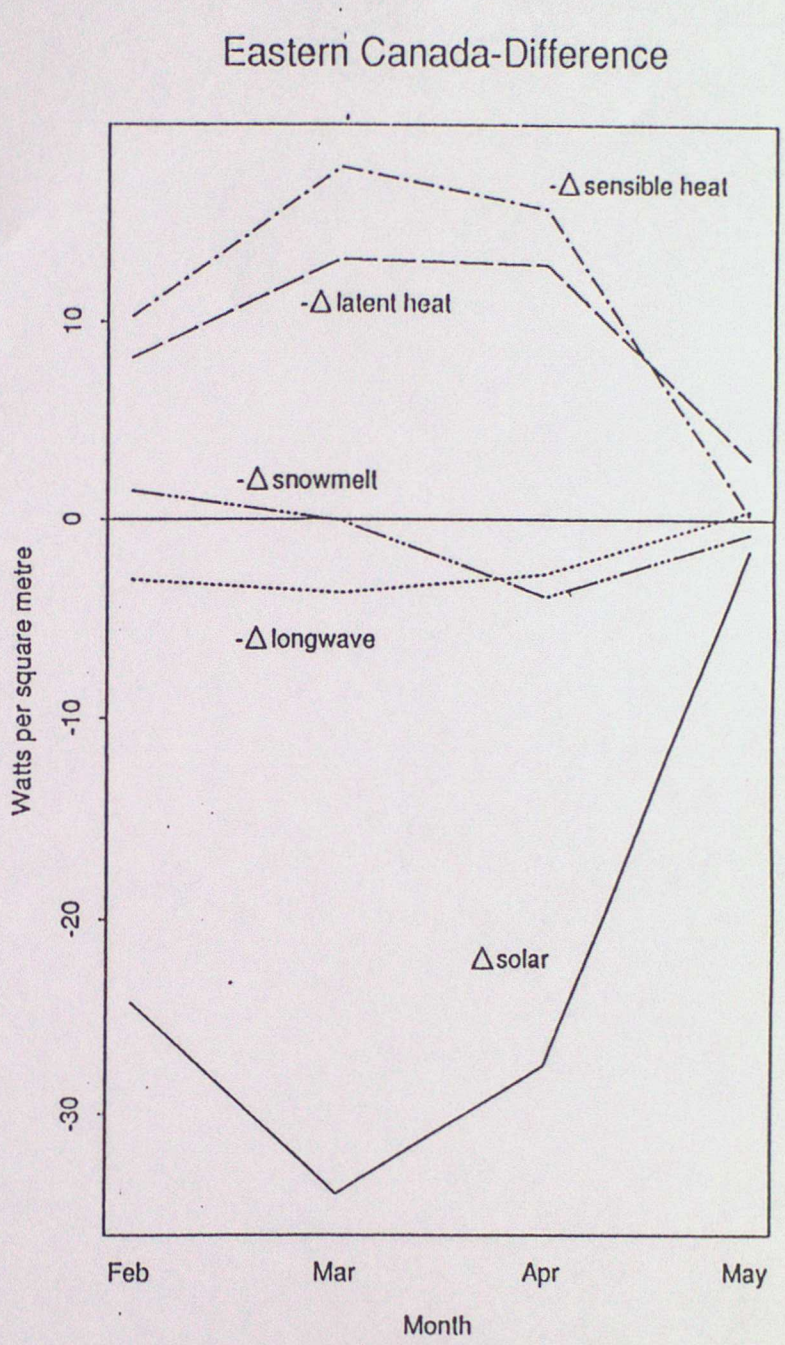

Figure 13b

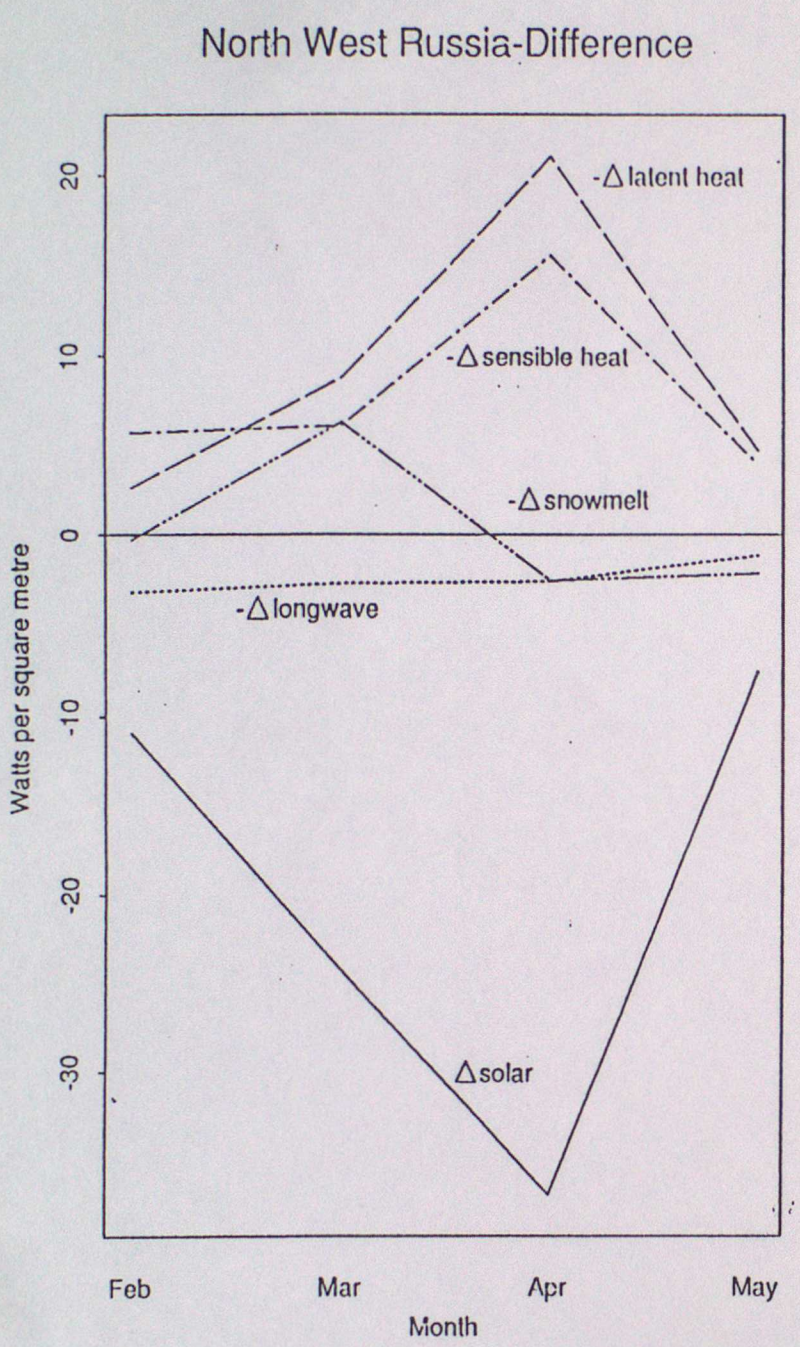

Figure 13c

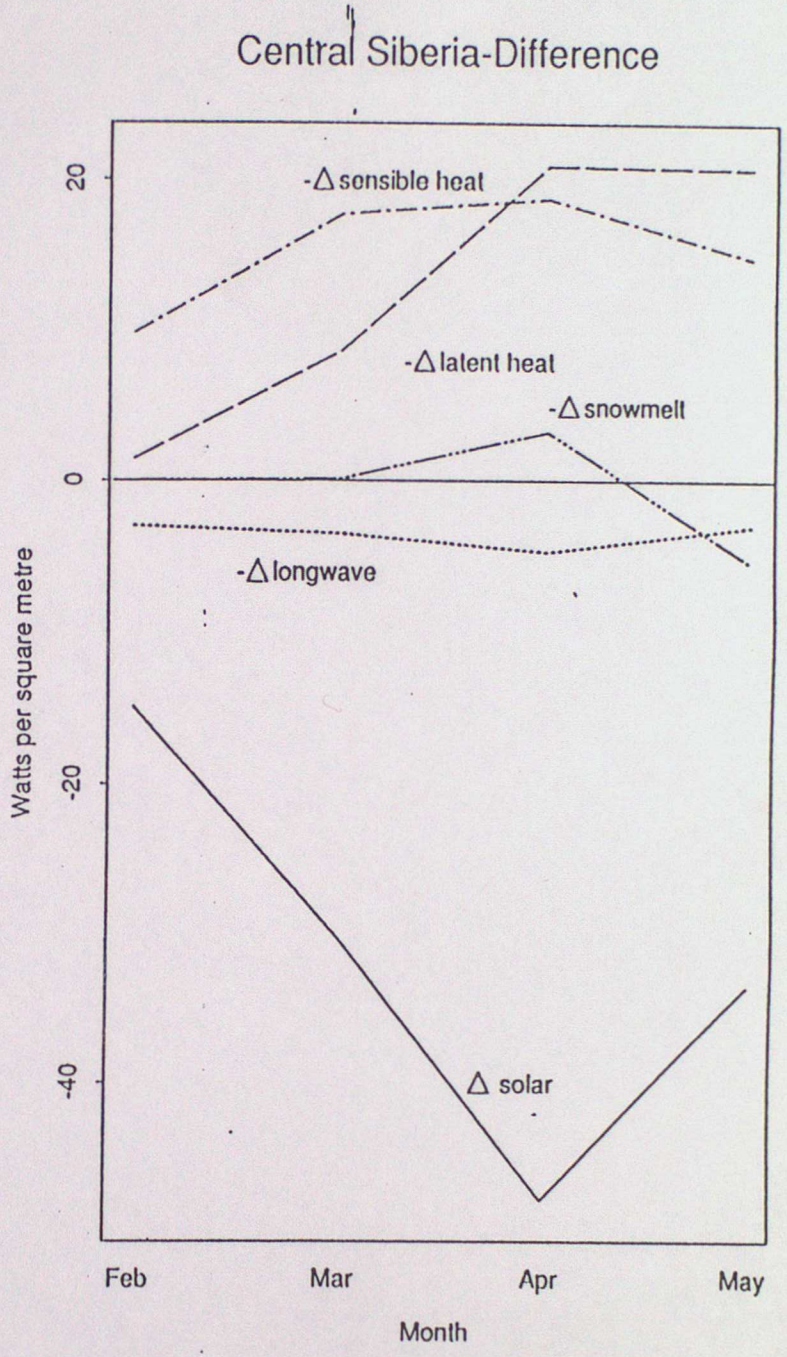

Figure 13d

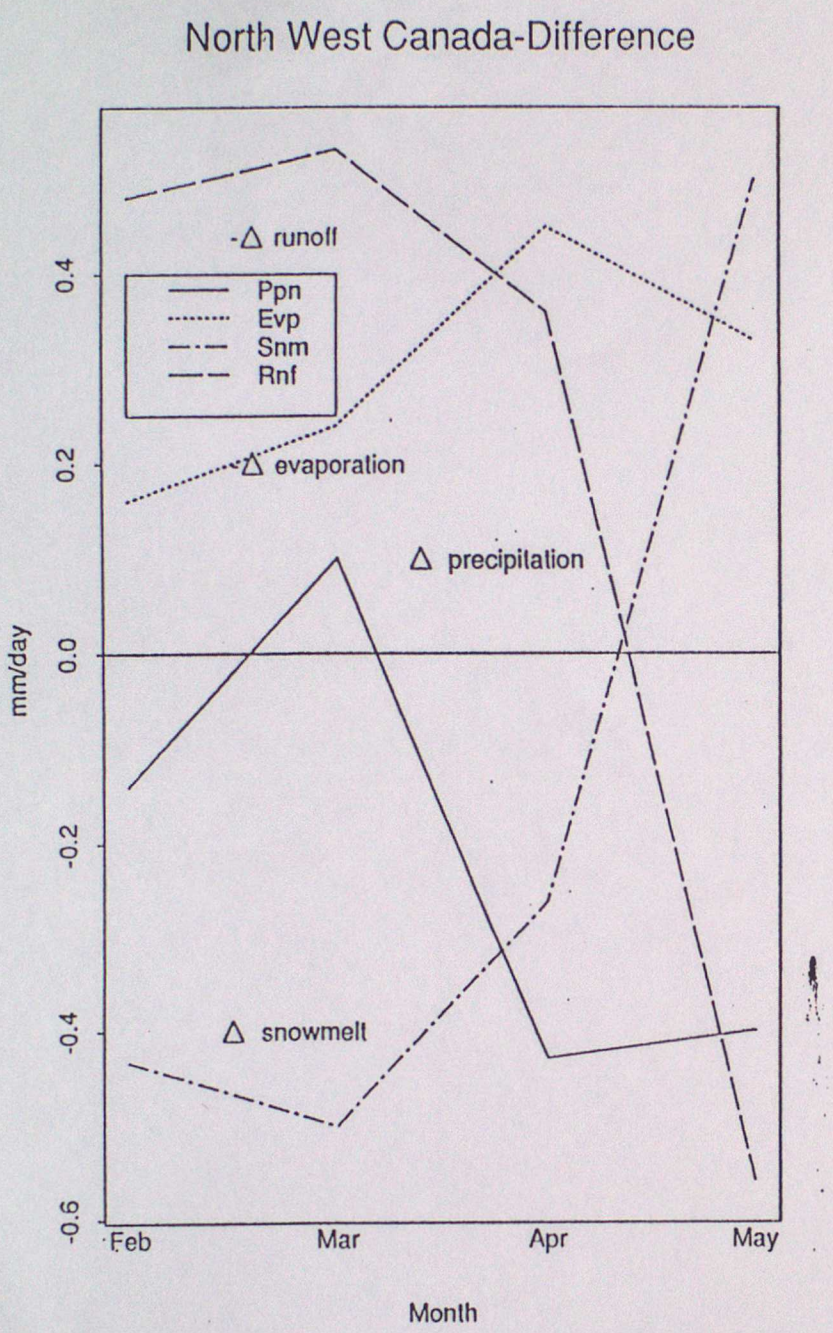

Figure 14a

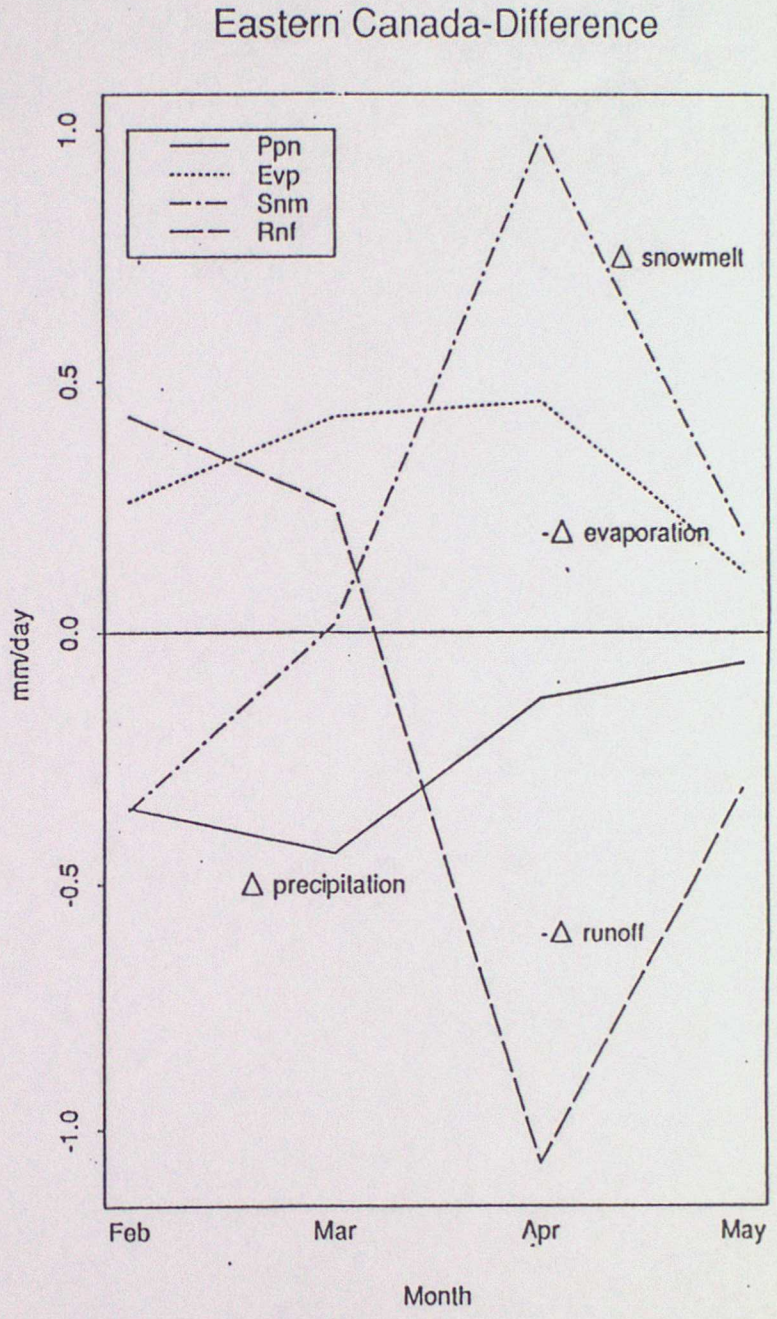

Figure 14b

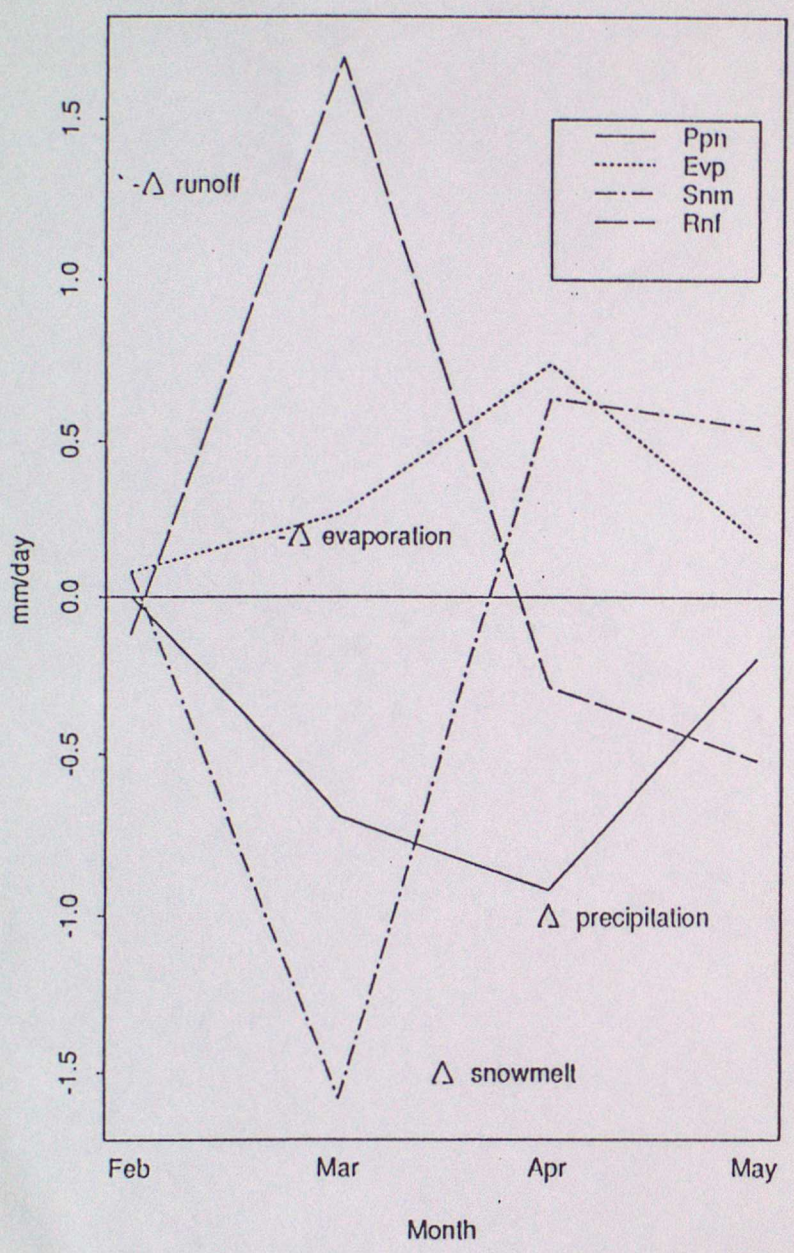

Figure 14c

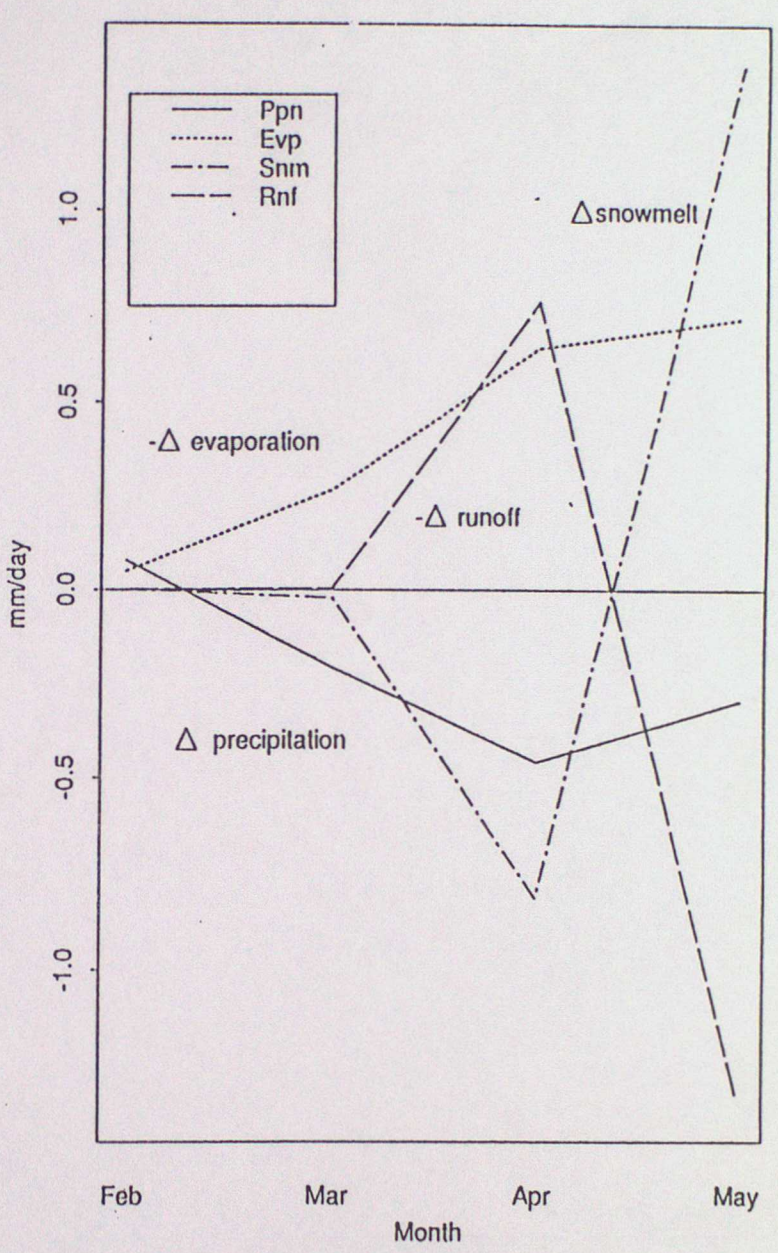

Figure 14d

CLIMATE RESEARCH TECHNICAL NOTES

CRTN 1	Oct 1990	Estimates of the sensitivity of climate to vegetation changes using the Penman-Monteith equation. P R Rowntree
CRTN 2	Oct 1990	An ocean general circulation model of the Indian Ocean for hindcasting studies. D J Carrington
CRTN 3	Oct 1990	Simulation of the tropical diurnal cycle in a climate model. D P Rowell
CRTN 4	Oct 1990	Low frequency variability of the oceans. C K Folland, A Colman, D E Parker and A Bevan
CRTN 5	Dec 1990	A comparison of 11-level General Circulation Model Simulations with observations in the East Sahel. K Maskell
CRTN 6	Dec 1990	Climate Change Prediction. J F B Mitchell and Qing-cun Zeng
CRTN 7	Jan 1991	Deforestation of Amazonia - modelling the effects of albedo change. M F Mylne and P R Rowntree
CRTN 8	Jan 1991	The role of observations in climate prediction and research. D J Carson
CRTN 9	Mar 1991	The greenhouse effect and its likely consequences for climate change. D J Carson
CRTN 10	Apr 1991	Use of wind stresses from operational N.W.P. models to force an O.G.C.M. of the Indian Ocean. D J Carrington
CRTN 11	Jun 1991	A new daily Central England Temperature series, 1772-1991. D E Parker, T P Legg and C K Folland
CRTN 12	Jul 1991	Causes and predictability of Sahel rainfall variability. D P Rowell, C K Folland, K Maskell, J A Owen, M N Ward
CRTN 13	Jul 1991	Modelling changes in climate due to enhanced CO_2, the role of atmospheric dynamics, cloud and moisture. C A Senior, J F B Mitchell, H Le Treut and Z-X Li

CLIMATE RESEARCH TECHNICAL NOTES

CRTN 14	Aug 1991	Sea temperature bucket models used to correct historical SST data in the Meteorological Office. C K Folland
CRTN 15	Aug 1991	Modelling climate change, and some potential effects on agriculture in the U.K. P R Rowntree, B A Callander and J Cochrane
CRTN 16	Aug 1991	The Boreal Forests and Climate G Thomas and P R Rowntree